Phycologia (2013) Volume 52 (6), 488–507 Published 5 December 2013

Ultrastructure and phylogeny of *Theleodinium calcisporum* gen. et sp. nov., a freshwater dinoflagellate that produces calcareous cysts

Sandra C. Craveiro[1,2]*, Mariana S. Pandeirada[1], Niels Daugbjerg[3], Øjvind Moestrup[3] and António J. Calado[1,2]

[1]*Department of Biology, University of Aveiro, P-3810-193 Aveiro, Portugal*
[2]*GeoBioTec Research Unit, University of Aveiro, P-3810-193 Aveiro, Portugal*
[3]*Marine Biological Section, Department of Biology, University of Copenhagen, Universitetsparken 4, DK-2100 Copenhagen Ø, Denmark*

Craveiro S.C., Pandeirada M.S., Daugbjerg N., Moestrup Ø. and Calado A.J. 2013. Ultrastructure and phylogeny of *Theleodinium calcisporum* gen. et sp. nov., a freshwater dinoflagellate that produces calcareous cysts. *Phycologia 52:* 488–507. DOI: 10:2216/13–152.1

A freshwater photosynthetic dinoflagellate isolated from a shallow lake near Aveiro, Portugal, was examined by light microscopy, scanning electron microscopy (SEM) and serial-section transmission electron microscopy (TEM), and characterized genetically. Cells were small, spherical to slightly elongated, and had a projecting, nearly cylindrical, apical pore. The chloroplasts were yellowish-brown, arranged near the surface of the cell, and had up to four pyrenoids surrounded by starch sheaths. The cells had a peridinioid plate pattern with Kofoidian plate formula pp, cp, x, 3′ (seldom 4′), 2a, 7′′, 6c, 5s (6s?), 5′′′, 2′′′′. A small extruded peduncle was observed by SEM in cells with intact membranes. A microtubular basket, made of about 46 microtubules disposed in four rows, was seen in the ventral area in connection with the cytoplasmic extension that made the peduncle. The flagellar apparatus was typical of a peridinioid with two roots associated with each of the basal bodies and a layered connective linking the proximal ends of roots 1 and 4. In dense cultures, this organism produced a round resting cyst with a thick wall covered by irregular calcified elements. Energy dispersive X-ray analysis (EDS) analysis of the cysts showed calcium as the most abundant element. A total of 3048 nucleotides of the nuclear ribosomal operon were sequenced and used in a phylogenetic analysis that placed this organism as a sister group to a clade of *Scrippsiella* species and the parasitic *Duboscquodinium collinii*. *Theleodinium calcisporum* gen. et sp. nov. is described for the first freshwater dinoflagellate reported to produce calcareous cysts.

Key Words: Calcareous cyst, Dinophyceae, ITS, LSU rDNA, Microtubular basket, Phylogeny, SSU rDNA, *Theleodinium* gen. nov., Ultrastructure

INTRODUCTION

Calcareous dinoflagellates have the capacity to produce calcified exoskeletal structures during at least one stage of their life cycle, usually a resting cyst stage derived from a zygote or perhaps from a vegetative cell (Gottschling *et al*. 2012). In the genus *Thoracosphaera* Kamptner the stage bearing a calcareous shell is instead interpreted as a vegetative, coccoid cell (Tangen *et al*. 1982). The presence of these calcareous structures has long been considered a synapomorphic character supporting the monophyly of this group of peridinioid dinoflagellates (Wall & Dale 1968). Calcareous forms are currently included in the family Thoracosphaeraceae together with some non-calcareous representatives, such as the pfiesterians, a group of versatile predators (e.g. *Pfiesteria* Steidinger & Burkholder, *Tyrannodinium* Calado, Craveiro, Daugbjerg & Moestrup), their close relatives (e.g. *Chimonodinium* Craveiro, Calado, Daugbjerg, Gert Hansen & Moestrup), and the parasite *Duboscquodinium collinii* Grassé (Elbrächter *et al*. 2008; Calado *et al*. 2009; Coats *et al*. 2010; Craveiro *et al*. 2011; Gottschling *et al*. 2012). These non-calcareous relatives are presumed to have secondarily lost the capacity to produce calcareous structures (Gottschling *et al*. 2005a, 2012).

* Corresponding author (scraveiro@ua.pt).

The external morphology of swimming cells of calcareous dinoflagellates is highly conserved; the theca comprises an apical pore, three series of epithecal plates and two series of hypothecal plates. The number of plates in major plate series is essentially constant; although, the number of plates in the cingulum varies between five and six (D'Onofrio *et al*. 1999; Gottschling *et al*. 2005b). Conversely, cyst morphology in this group of organisms is quite diverse and is important in species description and identification (Janofske 2000; Zinssmeister *et al*. 2012). The genus *Scrippsiella* Balech *ex* A.R. Loeblich comprises approximately 20 species of calcareous dinoflagellates, of which *Scrippsiella trochoidea* (F. Stein) A.R. Loeblich is the most commonly reported (Zinssmeister *et al*. 2011). *Scrippsiella trochoidea* has been suggested to represent a complex of cryptic species, with genetic differences not accompanied by differences in tabulation or in cyst morphology (D'Onofrio *et al*. 1999; Montresor *et al*. 2003; Gottschling *et al*. 2005b). Studies on the fine structure of calcareous dinoflagellates have been limited to vegetative swimming stages (Gao & Dodge 1991; Craveiro *et al*. 2011), vegetative coccoid stages of *Thoracosphaera heimii* (Lohmann) Kamptner (Tangen *et al*. 1982; Inouye & Pienaar 1983) and planozygote and calcareous cyst of *Scrippsiella* sp. (Gao *et al*. 1989). Recently, the ultrastructure of the cysts at an early development stage of several calcareous dinoflagel-

lates was examined to investigate the biomineralization process (Zinssmeister *et al*. 2013).

The classification of peridinioids was traditionally based on thecal features and was not supported by DNA-based phylogenetic hypotheses (Saldarriaga *et al*. 2004; Logares *et al*. 2007). The ultrastructural analysis of the type species of *Peridinium* Ehrenberg, *P. cinctum* (O.F. Müller) Ehrenberg, and *Peridiniopsis* Lemmermann, *P. borgei* Lemmermann, and the inclusion of these species in DNA-based phylogenetic hypotheses formed a base of comparison with other peridinioid species (Calado *et al*. 1999; Calado & Moestrup 2002; Moestrup & Daugbjerg 2007; Calado *et al*. 2009). Phylogenetic relationships of non-calcareous peridinioids have recently been addressed by combining information on external morphology, fine structure and DNA-based phylogenies (Calado *et al*. 2009; Craveiro *et al*. 2011). Recently, three new genera, *Parvodinium* Carty, *Palatinus* Craveiro, Calado, Daugbjerg & Moestrup and *Chimonodinium* were described to include three groups of species formerly included in *Peridinium sensu lato* (Carty 2008; Craveiro *et al*. 2009, 2011).

Peridinioid dinoflagellates producing calcareous cysts have previously been reported only from marine salinity regimes ranging from brackish waters in the Baltic Sea to highly saline waters of the Mediterranean Sea (Zonneveld *et al*. 2005). In this work, we describe a truly freshwater peridinioid that produced, in culture, cysts with an outer layer of irregular calcified crystals. We report on the morphology of swimming cell and cyst, the ultrastructure of the motile stage and a concatenated SSU, ITS and LSU rDNA-based phylogeny, and describe the organism as a new species of a new genus.

MATERIAL AND METHODS

The organism described herein was collected from a freshwater lake in Gafanha da Boavista, Ílhavo, Portugal on 2 March 2011. The conductivity, pH and water temperature measured during sampling were 323 µs/cm, 8.3 and 13.3°C respectively. Four motile cells that were lying on the bottom of an excavated slide were isolated into four wells with four times concentrated L16 medium (Linström 1991) supplemented with vitamins according to Popovský and Pfiester (1990). Three of these isolates grew into cultures that were maintained at 18°C with 12:12 light:dark photoperiod. All observations were made on these cultures.

Light micrographs of motile cells and cysts were taken with a Zeiss Axioplan 2 imaging light microscope (Carl Zeiss, Oberkochen, Germany) equipped with a DP70 Olympus camera (Olympus Corp., Tokyo, Japan). For SEM, cells were prepared according to three protocols that differed in the first fixation step. Protocol (1) was used to remove the outer membranes and visualize plate boundaries. Protocols (2) and (3) were used to preserve outer membranes, flagella and peduncle, with slightly better results in (3). In protocol (1) 0.5 ml of culture was fixed with 25% ethanol (final concentration) for 40 min; in (2) 0.6 ml of culture was fixed with an equal volume of a fixative mixture made of saturated $HgCl_2$ and 2% osmium tetroxide in a proportion of 1:5, for 10 min; in (3) 0.8 ml of culture was fixed with 0.4 ml of a fixative mixture made of saturated $HgCl_2$ and 2% osmium tetroxide in a proportion of 1:3, for 10 min. In all cases, fixation cells were collected onto 8 µm-pore Isopore polycarbonate membrane filters in Swinnex filter holders (Millipore Corp., Billerica, Massachusetts, USA), washed with distilled water for 30 min and dehydrated through a graded ethanol series. In protocol (1) the cells were critical-point-dried right after the dehydration. In protocols (2) and (3) cells stayed overnight in 100% ethanol before they were critical-point-dried. The dried filters were glued onto stubs, sputter-coated with gold-palladium and examined with a Hitachi S-4100 scanning electron microscope (Hitachi High-Technologies Corp., Tokyo, Japan).

Cysts were collected with a micropipette from the bottom of culture wells, transferred onto graphite-covered stubs and left to dry at room temperature. EDS of these uncoated cysts was performed in a Hitachi S-4100 scanning electron microscope (Hitachi High-Technologies Corp., Tokyo, Japan) equipped with a RONTEC EDS System with a UHV Dewar detector (Rontec GmbH, now Bruker Nano GmbH, Berlin, Germany).

Transmission electron microscopy (TEM)

For Transmission electron microscopy (TEM), swimming cells in culture were individually picked up, transferred to a mixture of 1% glutaraldehyde and 0.5% osmium tetroxide (final concentrations) in phosphate buffer 0.1 M, pH 7.2, and fixed for 20 minutes. After being washed in the same buffer, cells were embedded in 1.5% agar blocks and post-fixed overnight in 0.5% buffered osmium tetroxide. Following rinses in phosphate buffer and distilled water, the cells in the agar blocks were dehydrated through a graded ethanol series and propylene oxide, and embedded in Spurr's resin. The resin blocks were cured for about 14 hours at 70°C. Nine cells were sectioned with a diamond knife on an EM UC6 ultramicrotome (Leica Microsystems, Wetzlar, Germany). Ribbons of serial sections, about 70 nm thick, were picked up with slot grids and placed on Formvar film. After drying, the sections were stained with uranyl acetate and lead citrate. Serial sections of five cells were examined using a JEOL JEM 1010 transmission electron microscope.

DNA extraction and PCR amplification of ribosomal operon

For DNA extraction, 10 ml of a culture of *Theleodinium calcisporum* was centrifuged at 2500 rpm for 10 min at room temperature. Having discarded the supernatant the cell pellet was transferred to a 1.5 ml Eppendorf tube and placed at –20 °C until extraction of genomic DNA. For this we used the CTAB (hexadecyltrimethylammonium bromide) method as previously outlined in Daugbjerg *et al*. (1994). Amplification of the nuclear ribosomal operon (SSU rDNA, ITS 1, 5.8S rDNA and ITS 2 and approximately 700 nucleotides of LSU rDNA) was completed using three separate PCR reactions providing a total of 3048 nucleotides. PCR amplification of SSU and LSU rDNA was performed using primers ND1–ND6 and D1–ND28-1483, respectively (see table 1 in Hansen *et al*. 2007 for primer sequences). Chemicals

(including their concentrations) and temperature profile conditions for PCR amplification of SSU and LSU rDNA were identical to those described in Hansen *et al*. (2003). For sequence determination of ITS 1 and 2 including the 5.8S rDNA we used the common ITS1 and ITS4 primers designed by White *et al*. (1990). PCR amplification used the EmeraldAmp GT PCR Master Mix following the manufacturer's recommendations (TaKaRa Bio Inc, Shiga, Japan). Temperature profile: 1× (98°C), 35× (98°C for 10 s, 60°C for 30 s and 72°C for 1 min), 1× (72°C for 2 min). Expected lengths of DNA fragments were confirmed by electrophoresis using 1.5% agarose gels run for 20 min at 150 V. The gel contained ethidium bromide (SSU and LSU rDNA) or GelRed (ITS) and PCR fragments were viewed under a UV light table. Fragment lengths were compared to those of the molecular marker Phi X175 HAE III (ABgene, Rockford, IL, USA). PCR products were purified using the NucleoFast 96 PCR kit from Macherey-Nagel (GmbH & Co. KG, Düren, Germany), following the manufacturer's recommendations. 500 ng of air-dried PCR products were sent to Macrogen (Seoul, Korea) for sequence determination in both directions.

Alignment and phylogenetic analyses

For alignment and phylogenetic analyses, the ~3 k nucleotides determined in this study were added to an existing alignment compiled by Gottschling *et al*. (2012). This data matrix included a diverse assemblage of dinoflagellates (118 taxa and 37 genera) and a total of 4618 positions including introduced gaps. It was used to infer the phylogeny of Thoracosphaeraceae and is available at http://datadryad.org/handle/10255/dryad.33663 as file Fig02.nex. The data matrix analyzed here thus contained 119 taxa and 4620 positions, and we used Jalview (ver. 2.8) for sequence editing (Waterhouse *et al*. 2009). The ingroup of dinoflagellates were rooted using three apicomplexans and two species of *Perkinsus*. MrBayes (v. 3.2, Ronquist & Huelsenbeck 2003) was used to perform Bayesian analysis with a general time reversible substitution model. In an attempt to more accurately model sequence evolution of the ribosomal operon we divided the data into five partitions (i.e. SSU rDNA, ITS 1, 5.8S rDNA, ITS 2 and LSU rDNA), thus allowing each of these regions to have evolved under different models of evolution by using the 'unlink' option. Two independent Markov Chain Monte Carlo (MCMC) (each comprising one cold and three heated chains) were run for 2×10^6 generations. Parameter values and trees were sampled and saved every 200th generation. With Microsoft Excel we plotted the log likelihood values as a function of generations. The lnL values converged at ca. –89,313.7 after 80,200 generations. This left 9600 trees and these were imported into PAUP* (Swofford 2002) to produce a 50% majority rule consensus tree. Posterior probabilities (pp) were also obtained from the 9600 trees and the values added to the tree topology. Maximum likelihood analyses were performed using PhyML (Guindon *et al*. 2010). For this we used the parameter settings suggested by Modeltest (v. 3.7, Posada & Crandall 1998) with gamma shape G = 0.42 and proportion of invariable sites I = 0.18. We used 500 bootstrap replications in maximum likelihood to evaluate the robustness of the tree topology. PhyML was run via the online version freely available at the Bioportal, University of Oslo. We used PAUP* to calculate sequence divergence estimates.

A phylogeny based on ITS 1, 5.8S rDNA and ITS 2 was used to further explore the phylogeny of *Theleodinium calcisporum*; we compiled a second data matrix similar to Zinssmeister *et al*. (2012). It included a higher number of supposedly closely related dinoflagellates such as *Calciodinellum* spp. (three species), *Pernambugia tuberosa* (Kamptner) Janofske & Karwath and eight additional species of *Scrippsiella* compared to the diversity included in Figs 61 and S1 (online). The 'ITS 1–5.8 S rDNA–ITS 2′ data matrix with 655 nucleotides (including introduced gaps) was analyzed using Bayesian analysis with division into three partitions (see above) and maximum likelihood, with an ingroup of 24 taxa and *Peridinium cinctum* as the outgroup. The alignment was generated using Clustal W as implemented in Jalview ver. 2.8 (Waterhouse *et al*. 2009). In Bayesian analysis we ran 2×10^6 generations and the burn-in was obtained after 20,200 generations (print frequency = 200). This left 9900 trees for a 50% majority rule consensus tree. For maximum likelihood analysis we used PhyML with settings of gamma shape G = 1.16 and proportion of invariable sites I = 0.404 as suggested by jModelTest ver. 2.1.3 (Darriba *et al*. 2012). Bootstrap analyses included 1000 replications. The PhyML analysis was run through the South of France bioinformatics platform.

RESULTS

Theleodinium Craveiro, Pandeirada, Daugbjerg, Moestrup & Calado *gen. nov.*

DESCRIPTION: Free-living photosynthetic dinoflagellate; amphiesma of motile cells with well-developed plates arranged in a peridinioid pattern; Kofoidian plate formula typically pp, cp, x, 3′, 2a, 7′′, 6c, 5s (6s?), 5′′′, 2′′′′, the number of apical plates occasionally up to four (through division of plate 2′); apical pore projecting, nipple-like; small extruded peduncle present, supported by a microtubular basket of three or four rows of microtubules and accompanied by electron-opaque, elongated vesicles in its distal part; pusular system with flattened, convoluted tubes wrapped in a vesicle, on the right-ventral side of the cell, connected with the longitudinal flagellar canal; pyrenoids present; theca opening along the upper edge of the cingulum; resting cyst with a thick wall covered by calcified elements.

TYPE SPECIES: *Theleodinium calcisporum* Craveiro, Pandeirada, Daugbjerg, Moestrup & Calado *sp. nov.*

ETYMOLOGY: Greek θηλή, "nipple", from the shape of the apical protuberance. The termination *–dinium*, originally from Greek δινη, "vortex", is common in dinoflagellate generic names.

Theleodinium calcisporum Craveiro, Pandeirada, Daugbjerg, Moestrup & Calado *sp. nov.*

Figs 1–26

DESCRIPTION: Motile cells small, 16–25 μm long and 13–23 μm wide, globose or slightly flattened dorsoventrally; roundish cells, epi- and hypocone of similar size; plates with scattered trichocyst pores but otherwise smooth; chloroplasts yellowish-brown with the lobes arranged mainly near the surface of the cell; three or four starch-enveloped pyrenoids penetrated by thylakoids; eyespot absent; nucleus located dorsally at cingulum level; resting cyst round, with calcified outer layer made of variable crystalline elements, sometimes

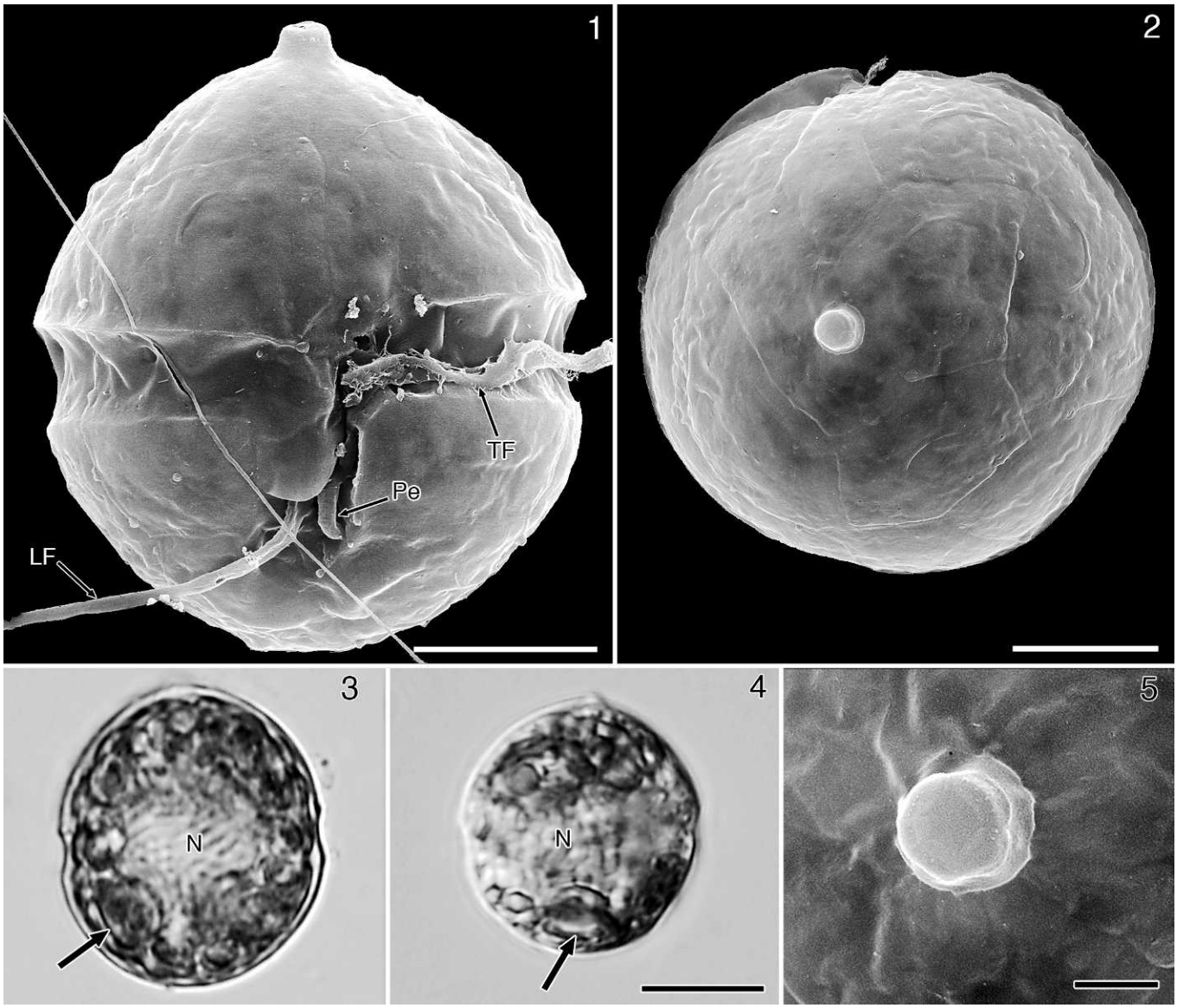

Figs 1–5. *Theleodinium calcisporum,* SEM and LM.
Fig. 1. Ventral view of a cell with preserved outer membranes, flagella and peduncle (SEM). The proximal part of the transverse flagellum (TF) is visible in the cingulum. The longitudinal flagellum (LF) emerges in the sulcus, on the right side of a small peduncle (Pe). Scale bar = 5 μm.
Fig. 2. Apical view of a cell with preserved membranes (SEM). The ventral side of the cell is facing the top of the image. The central protuberance corresponds to the apical pore. Scale bar = 5 μm.
Figs 3, 4. Longitudinal views of two cells in LM showing the central nucleus (N) and the chloroplast lobes with pyrenoids (arrows). Scale bar = 10 μm.
Fig. 5. Higher magnification of the apical pore of the cell in Fig. 2 (SEM). Scale bar = 1 μm.

up to 25 μm thick but mostly 1–2 μm thick, paratabulation not visible; living in freshwater; nuclear-encoded SSU, ITS and partial LSU rRNA gene sequence = GenBank accession KC699492.

HOLOTYPE: SEM stub with critical point dried material, with flagella and outer membranes removed, showing thecal plates, deposited at the University of Aveiro Herbarium registered as AVE-A-T-2. Figures 6–10 and 15–17 illustrate cells from this stub, and Figs 11–14 summarize the main surface features of this material.

ISOTYPE: Graphite-covered SEM stub with air-dried, uncoated material from the same clonal culture as the holotype, with calcified cysts used for EDS analysis and some collapsed cells, deposited at the University of Aveiro Herbarium registered as AVE-A-T-3.

TYPE LOCALITY: Freshwater, shallow lake in Gafanha da Boavista, Ílhavo, Portugal (40°36′13.54″N, 8°41′49.17″W), type collected on 2 March 2011.

ETYMOLOGY: *Calcisporum* (Latin = calcified spore) refers to the resting cysts with a layer of calcified crystals outside the organic cell wall.

Cells were spherical to slightly elongated, not compressed or only slightly compressed dorsoventrally (Figs 1–4). The

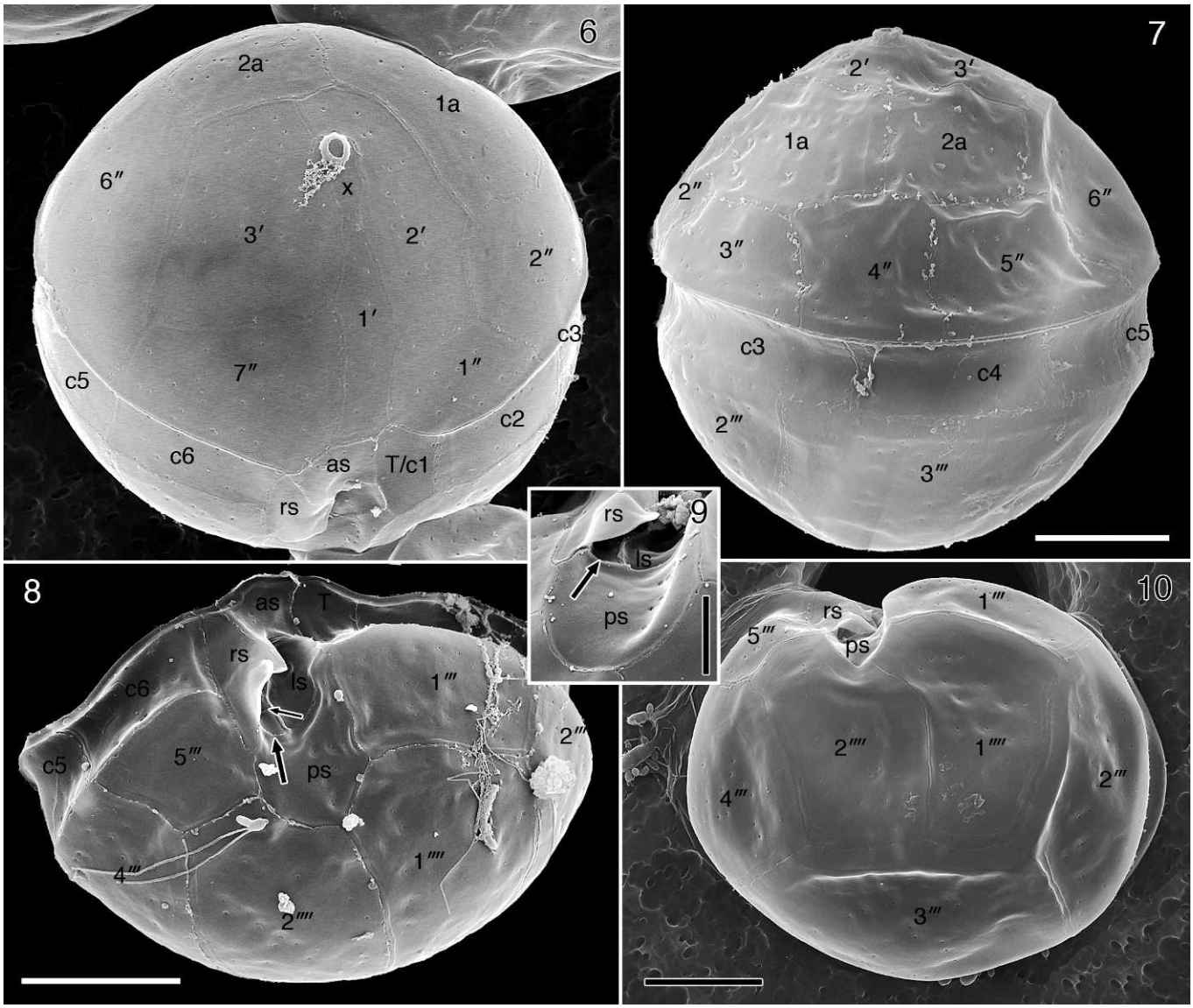

Figs 6–10. *Theleodinium calcisporum*, SEM. Plates are labelled in Kofoidian notation.
Fig. 6. Ventral-apical view showing the three apical and the two anterior intercalary plates. The first, narrow cingular plate, partly located in the sulcal area, is marked T/c1. Same scale as Fig. 7.
Fig. 7. Dorsal view showing intercalary plates and the dorsal plates of the precingular, cingular and postcingular series. Scale bar = 5 μm.
Fig. 8. Ventral-antapical view of the hypotheca. Anterior (as), right (rs), left (ls) and posterior (ps) sulcal plates. Two accessory sulcal plates are partly visible under the raised left side of the rs: the larger arrow points to the suture between the ps and the posterior accessory plate and the smaller arrow indicates the suture between the two accessory sulcal plates. Scale bar = 5 μm.
Fig. 9. Detail of sulcal area. The arrow indicates the accessory sulcal plate. Scale bar = 2 μm.
Fig. 10. Antapical view showing two antapical plates of similar size and five postcingular plates. Scale bar = 5 μm.

cingulum was located equatorially with a minor downward shift at the distal end, dividing the cell into similar-sized, hemispherical epi- and hypocone (Figs 1, 3, 4). The cell apex shows a projecting, almost cylindrical, apical pore, 1.0–1.1 μm long and 1.2–1.5 μm wide (Figs 1, 5). The sulcus did not invade the epitheca. Length of cells varied between 16 and 25 μm and width between 13 and 23 μm ($n = 45$), length:width ratio 1.0–1.3. A small extruded peduncle, ca. 2 μm long and 0.5 μm wide, was visible in SEM in cells that retained the outer membranes and flagella (Fig. 1).

The brown chloroplast lobes were located near the cell surface; up to four large pyrenoids surrounded by starch sheaths were present in the cell (Figs 3, 4). The nucleus was located at cingulum level in the mid-dorsal side of the cell (Figs 3, 4).

Plate tabulation is shown in SEM (Figs 6–10) and is represented in the schematic drawings of Figs 11–14. Epithecal tabulation was unusual and somewhat variable. Only three apical plates were usually found surrounding the apical pore complex (Figs 6, 11–13, 15, 16). In the most common plate organization the first apical plate was thin and elongated, while the second apical plate was almost rectangular and extended around the left-dorsal side of the apical pore complex to contact the wider apical plate 3 on

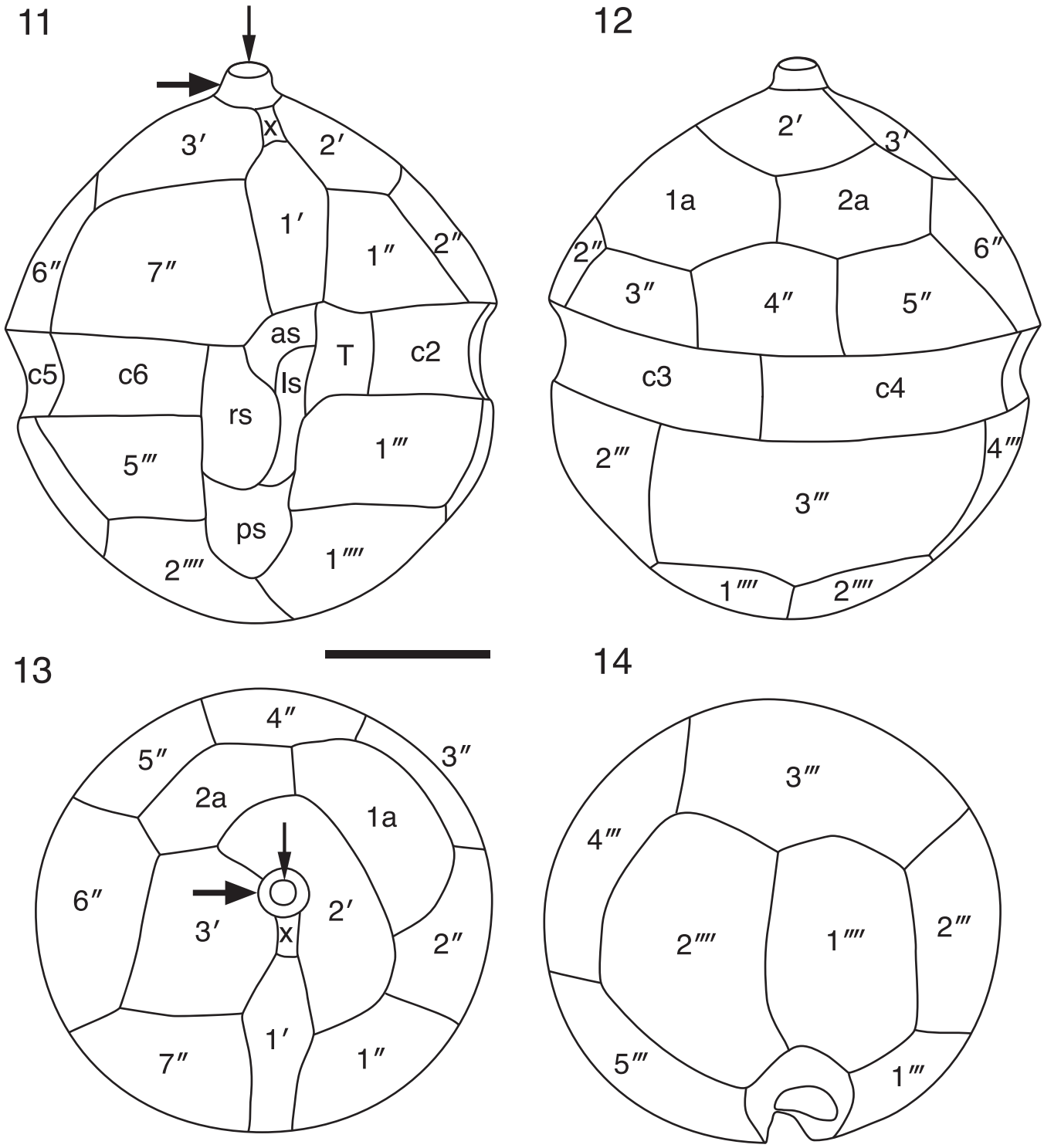

Figs 11–14. *Theleodinium calcisporum*, schematic drawings showing morphology and plate arrangement. Plates are labelled in Kofoidian notation. The thin arrow points to the cover plate (cp) and the thick arrow to the pore plate (pp); x marks the canal plate. Scale bar = 5 μm. Figures 11–14 represent ventral, dorsal, apical and antapical views, respectively.

the dorsal-right side of the cell (Figs 6, 13, 15). Two anterior intercalary plates were present in the dorsal side, with plate 1a usually larger than 2a (Figs 6, 7, 12, 13). The number of precingular plates was consistently seven (Figs 6, 7, 11–13); precingular plates 1 to 5 were usually smaller than precingular plates 6 and 7 (Figs 6, 13). The apical pore complex was made of three platelets; the canal plate (marked x in Figs 6, 11, 13, 15–17) was rectangular (1.4–2 μm long) or sometimes a little wider toward the pore plate (up to 1 μm wide) than toward apical plate 1 (0.6–1 μm wide); the round

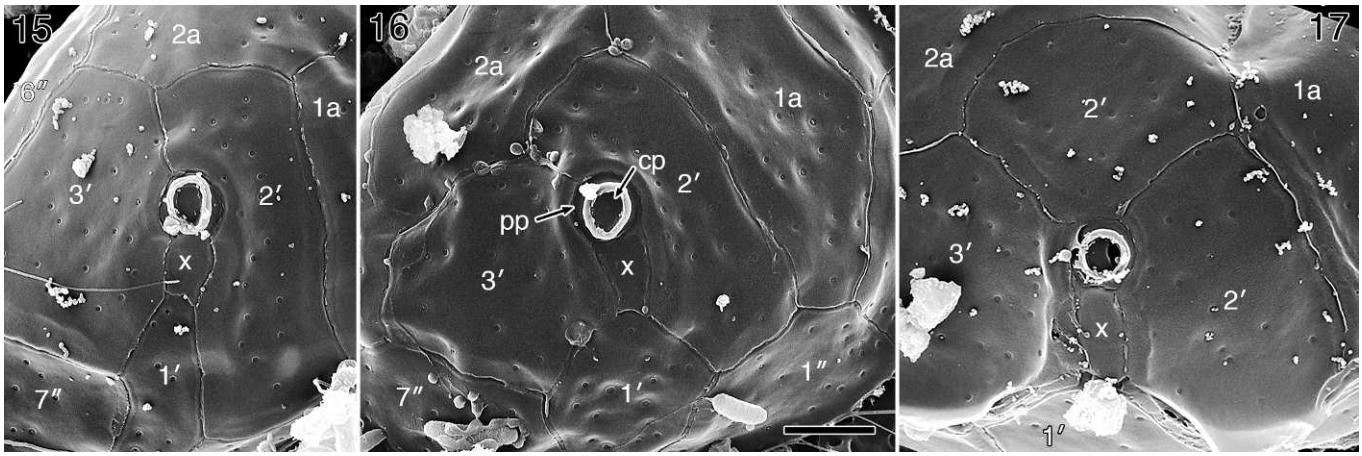

Figs 15–17. *Theleodinium calcisporum*, variation in number and shape of apical plates. Plates are labelled in Kofoidian notation; x, canal plate; cp, cover plate; pp, pore plate. Scale bar = 2 μm.
Fig. 15. First apical plate narrow.
Fig. 16. First apical plate rhombic.
Fig. 17. Apical plate 2 divided into two, forming a symmetrical arrangement around the apical pore.

pore plate (pp), which was usually collapsed in cells without the outer membranes and resembled a thick ring (Figs 6, 15–17); and the small cover plate (cp; diameter ca. 0.8 μm) (Figs 6, 13, 15–17). In the cingulum there were six plates. The first cingular plate was short and its right side invaded the sulcal area; plates in this position are usually called transitional (labelled T in Figs 6, 8, 11). The hypotheca had five postcingular and two antapical plates of similar size (Figs 8, 10, 14). Five plates were regularly seen in the sulcus (Figs 8, 9, 11): the anterior sulcal plate (as), the right (rs) and left (ls) sulcal plates, the posterior sulcal plate (ps) and an intermediate, smaller plate, partially covered by the raised left border of the right sulcal plate, here called accessory sulcal plate (large arrow in Figs 8, 9). The small arrow in Fig. 8 points to what seems to be a suture, indicating the possible presence of two accessory plates in an anterior-posterior alignment under the border of rs, which would correspond to a total of six sulcal plates.

Variation to the general tabulation type described above was found in the cultures, mainly affecting the shape and number of apical plates. The first apical plate varied from very narrow and almost linear (Figs 6, 11, 13, 15) to wider and more rhombic (Figs 16, 17). Another important variation was seen in apical plate 2, which was divided into two plates in about 13% ($n = 23$) of the cells in culture (Fig. 17).

The surfaces of all plates were completely smooth and perforated by small circular pores (probably trichocyst pores) randomly distributed (Figs 6–10). Sutures between plates were mostly very narrow and when a little wider they were not ornamented (Fig. 10). The theca opened along the upper edge of the cingulum for releasing dividing or ecdysing cells (Figs 8, 10).

Cysts were observed for the first time in 24-well tissue culture plates, in cultures about three months old. Although large numbers of cysts were commonly found on the bottom of old cultures kept in wells, cyst formation was not detected in cultures maintained in 50-ml tissue culture flasks, perhaps because cell density was always smaller in these larger volumes. Cysts were round to slightly elongate with 17.1–29.6 μm in diameter ($n = 15$; Figs 18–23, 25). Cyst contents were usually colourless with the exception of one or two large red or orange bodies (Fig. 20). The cyst wall consisted of a layer of apparently crystalline elements (Figs 18, 19, 21–26) covering a thick, presumably organic layer (Fig. 20). The crystals were sometimes few, small and almost cubic, scattered along the cyst surface (Figs 22–24). The most common cyst type had the entire surface covered by larger crystalline elements, angular or irregular in shape and arrangement (Fig. 18), or by irregular but round-edged crystals (Figs 19, 25, 26). In yet other cases the cysts were very large, up to 60 μm diameters, and the crystal elements were difficult to separate from each other (Fig. 21). Some cysts had an opening with an irregular shape, perhaps representing the archeopyle formed during cyst germination (Fig. 25). No sign of paratabulation was observed.

The calcareous nature of the cyst wall was tested by adding a drop of 45% acetic acid to cysts like the one in Fig. 19 under the light microscope. Within seconds to a few minutes, the cysts lost all the crystal elements and showed a smooth wall about 1 μm thick (Fig. 20). Analysis of crystal-covered cysts by EDS showed calcium as the most abundant element (Fig. 27).

The internal fine structure of the cell was typical of dinoflagellates. General cell views are shown in longitudinal-tangential and transverse sections of two cells in Figs 28 and 29. The chloroplast lobes were located predominantly near the cell surface and had some thylakoid-free areas; the ellipsoid nucleus (N) was located on the dorsal side of the cell (Fig. 29). Although chloroplasts had typically three thylakoids per lamella, arrangements of five or six thylakoids per lamella and larger, almost granum-like stacks were also observed (Figs 30, 31). Up to four large starch-covered pyrenoids (P) per cell were found (Figs 28, 29). Several chloroplast lobes radiated from each pyrenoid (Fig. 28). Pyrenoids were penetrated by two-thylakoid lamellae (arrows in Figs 30, 32). Oil droplets (O) and starch grains (S) were distributed in the cell cytoplasm (Figs 28, 29). Trichocysts were widely scattered over the cell cytoplasm

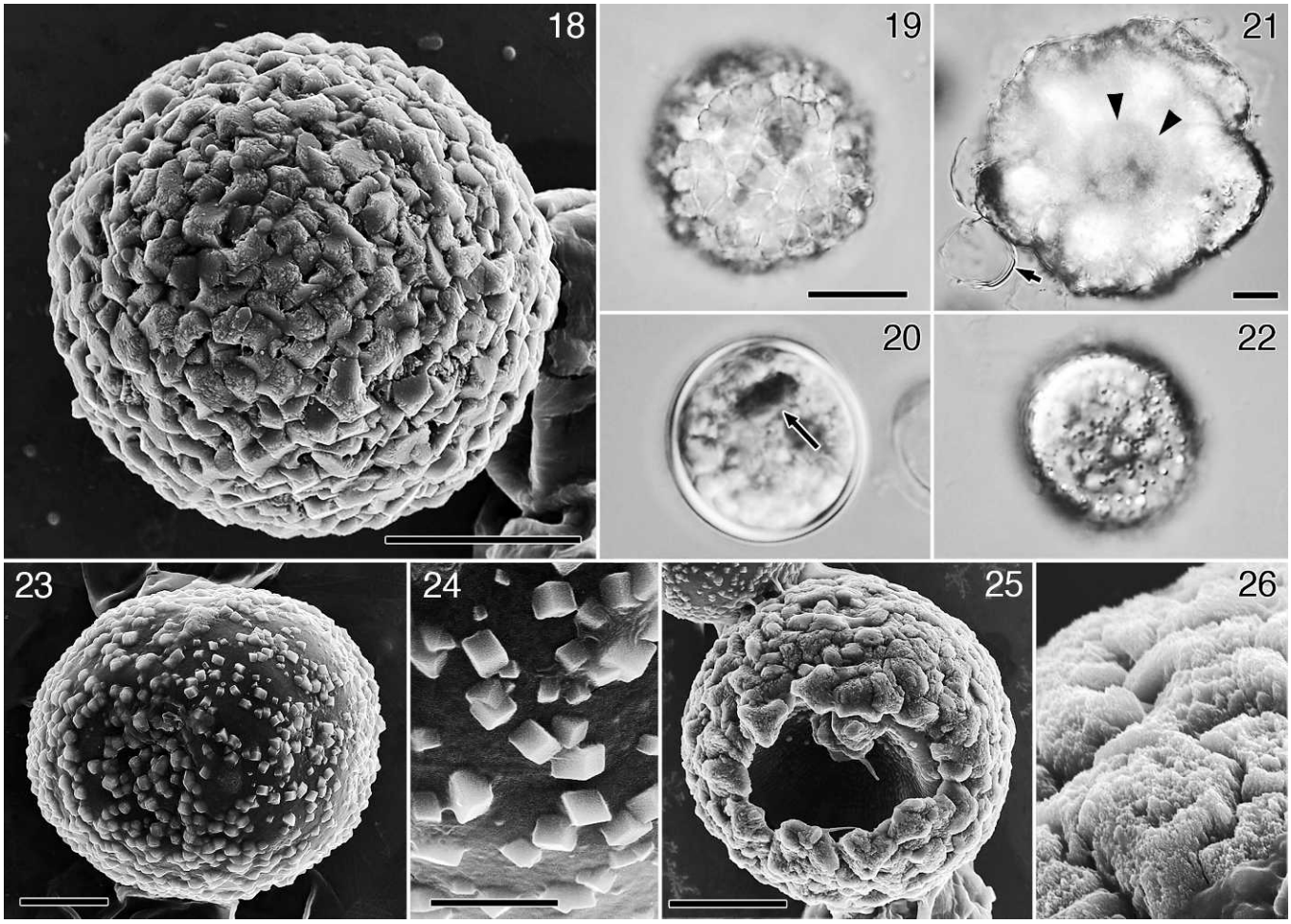

Figs 18–26. *Theleodinium calcisporum*, cysts, SEM and LM.
Fig. 18. Round cyst with well-developed crystals of irregular shape, SEM. Scale bar = 10 μm.
Fig. 19. Cyst with well-developed crystals, LM. Scale bar = 10 μm.
Fig. 20. Same specimen as in Fig. 19, with round, smooth wall after dissolution of calcified layer through the addition of 45% acetic acid. The arrow indicates coloured body. Same scale as Fig. 19.
Fig. 21. Cyst with very thick layer of crystals, LM. Arrowheads point to the cell in the central part of the cyst. The arrow indicates the remnants of a theca. Scale bar = 10 μm.
Fig. 22. Cyst with small crystals dispersed on the organic wall, LM. Same scale as Fig. 19.
Fig. 23. Cyst with small cubic crystals dispersed on the organic wall, similar to the one in Fig. 22, SEM. Scale bar = 5 μm.
Fig. 24. Detail of the cubic crystals in Fig. 23, SEM. Scale bar = 2 μm.
Fig. 25. Cyst with large irregular crystals and an opening (archeopyle?), SEM. Scale bar = 10 μm.
Fig. 26. Detail of crystals of a cyst similar to the one in Fig. 25, perhaps representing a more developed stage, SEM. Same scale as Fig. 23.

(Fig. 28, t). One or two accumulation bodies were found in the epicone of all cells examined (not shown). No eyespot was seen in the sulcal area of the cells observed.

Longitudinal sections through the apical pore complex showed the pore plate with three zones of different aspect inside the same amphiesmal vesicle: a basal zone, with the same appearance as other thecal plates; a more fibrous-looking middle zone that formed the raised side of the apical pore; and a third small zone with a darker fibrous aspect on the apical side of a section through the middle of the structure (Figs 33–36). The cover plate (cp) was about 0.5 μm thick and had also a fibrous aspect (Figs 33, 34).

The pore and cover plates were underlain by a more or less compact fibrous layer. Several distinct fibres extended from the central, compact fibrous layer (arrowheads in Figs 33–

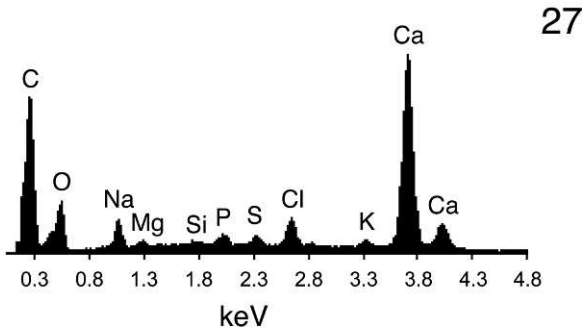

Fig. 27. Spectrum obtained from elemental EDS microanalysis of a *Theleodinium calcisporum* cyst. The peaks are labelled with the EDS line of the corresponding element.

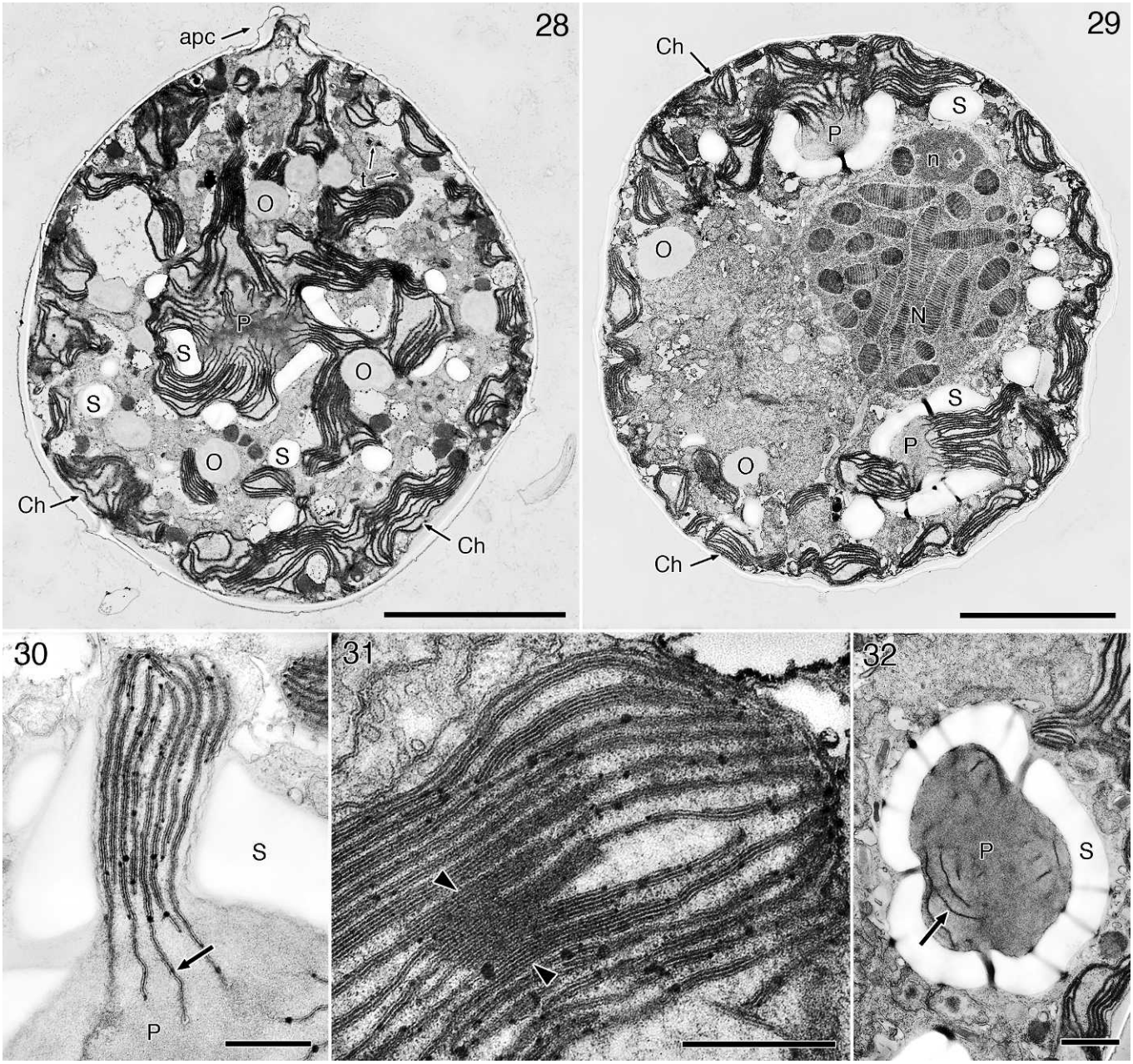

Figs 28–32. *Theleodinium calcisporum*, general ultrastructural features, TEM.
Fig. 28. Oblique longitudinal section of a cell viewed from the dorsal-right side showing the apical pore complex (apc), the chloroplast lobes (Ch) near the cell surface, one pyrenoid (P) and the distribution of oil droplets (O), starch (S) and trichocysts (t). Scale bar = 5 μm.
Fig. 29. Approximately transverse section through the middle part of the cell (antapical view). The nucleus (N) with a nucleolus (n) is on the dorsal side. Two pyrenoids (P) are visible on peripheral chloroplast lobes (Ch). O, oil droplets; S, starch. Scale bar = 5 μm.
Fig. 30. Pyrenoid (P) matrix penetrated by thylakoid lamellae (arrow). Starch grains (S) surround the pyrenoid. Scale bar = 500 nm.
Fig. 31. Chloroplast lobe showing thylakoid lamellae in groups of three or four. In the central part a pseudogranum-like stack of thylakoids (arrowheads). Scale bar = 500 nm.
Fig. 32. Section through the pyrenoid (P) matrix completely surrounded by starch (S). Portions of thylakoid lamellae are visible inside (arrow). Scale bar = 1 μm.

36) and continued under the canal plate and apical plates 2 and 3 for at least 0.5 μm (not shown).

The pusular system was composed of convoluted, somewhat flattened tubes wrapped in a vesicle, located on the right-ventral side of the cell, near the basal bodies (Figs 37, 38). No clear ramifications of pusular elements were demonstrated. Two tubes seemed to connect to the longitudinal flagellar canal, which appeared collapsed in all cells examined (Figs 39–41): one tube was about 100 nm wide near the connection to the flagellar canal, where the three pusular membranes were closely appressed (Fig. 40, white arrow); the zone of apparent connection of the other tube was wider (ca. 300 nm) and occurred next to a layer of parallel fibril-like structures nearly 30 nm apart from each

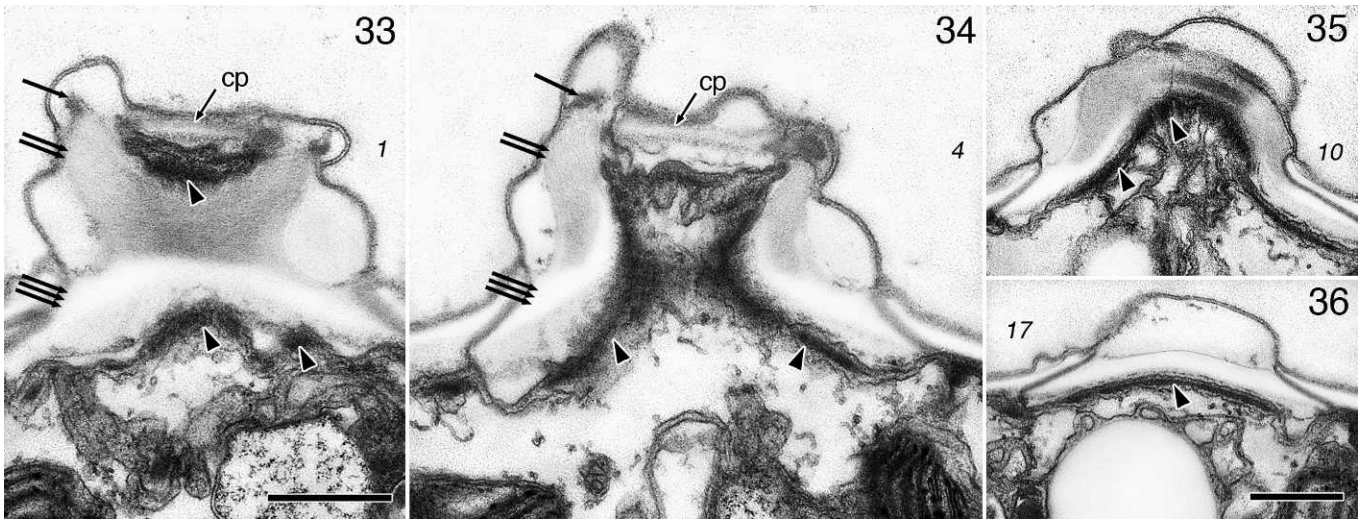

Figs 33–36. *Theleodinium calcisporum*, apical pore complex, TEM. Non-adjacent, serial longitudinal sections viewed from the dorsal-right side of the cell. Slanted numbers represent section numbers.

Fig. 33. Tangential section through the pore plate showing three different parts: the basal part with the white general aspect of other plates (three thin arrows), a medium part with a more fibrous aspect (two thin arrows) and a darker apical part (one thin arrow). The cover plate (cp) is covering the whole of the pore plate. Several fibers are seen under both the cover and pore plates (arrowheads). Scale bar = 500 nm.

Fig. 34. Section through the cover plate (cp) and pore plate with its three different-looking zones indicated as explained in Fig. 35. Fibers marked with arrowheads. Same scale as Fig. 35.

Figs 35–36. Fibers under the ventral-left side of the pore plate, marked with arrowheads. Scale bar = 500 nm, serves both figures.

other (Fig. 41). No pusular elements were found connecting to the transverse flagellar canal.

A schematic reconstruction of the flagellar apparatus structures found in the ventral area, as seen from the left side of the cell, is presented in Fig. 39. This includes the peduncle and its associated microtubules (microtubular basket, MB), the basal bodies and associated roots, collars and pusular elements. In the series presented in Figs 40–48 these components are seen approximately from the right-antapical side of the cell and in Figs 49–51 from the right-dorsal side. In Figs 52–55 a detail of this area is shown in an almost ventral view.

The transverse (TB) and longitudinal (LB) basal bodies formed an angle of about 80°–90°, as estimated from the reconstruction of the serial sections. Both longitudinal and transverse flagella exited from the flagellar canals to the exterior of the cell through pores encircled by complete rings of fibrous material called longitudinal (LSC) and transverse

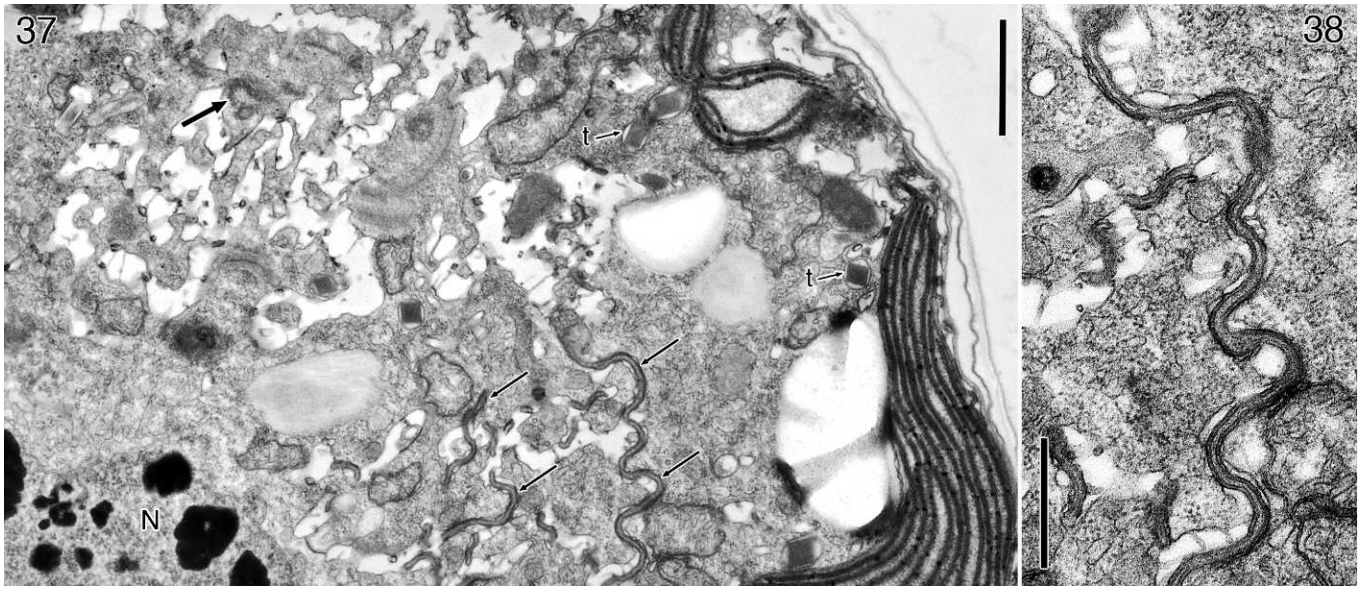

Figs 37–38. *Theleodinium calcisporum*, pusular system, TEM.

Fig. 37. Transverse section of a cell (apical view) showing pusular tubes (thin arrows) near the ventral area where a basal body (thick arrow) is seen. N, nucleus; t, trichocyst. Scale bar = 1 μm.

Fig. 38. Higher magnification of a pusular tube. Scale bar = 500 nm.

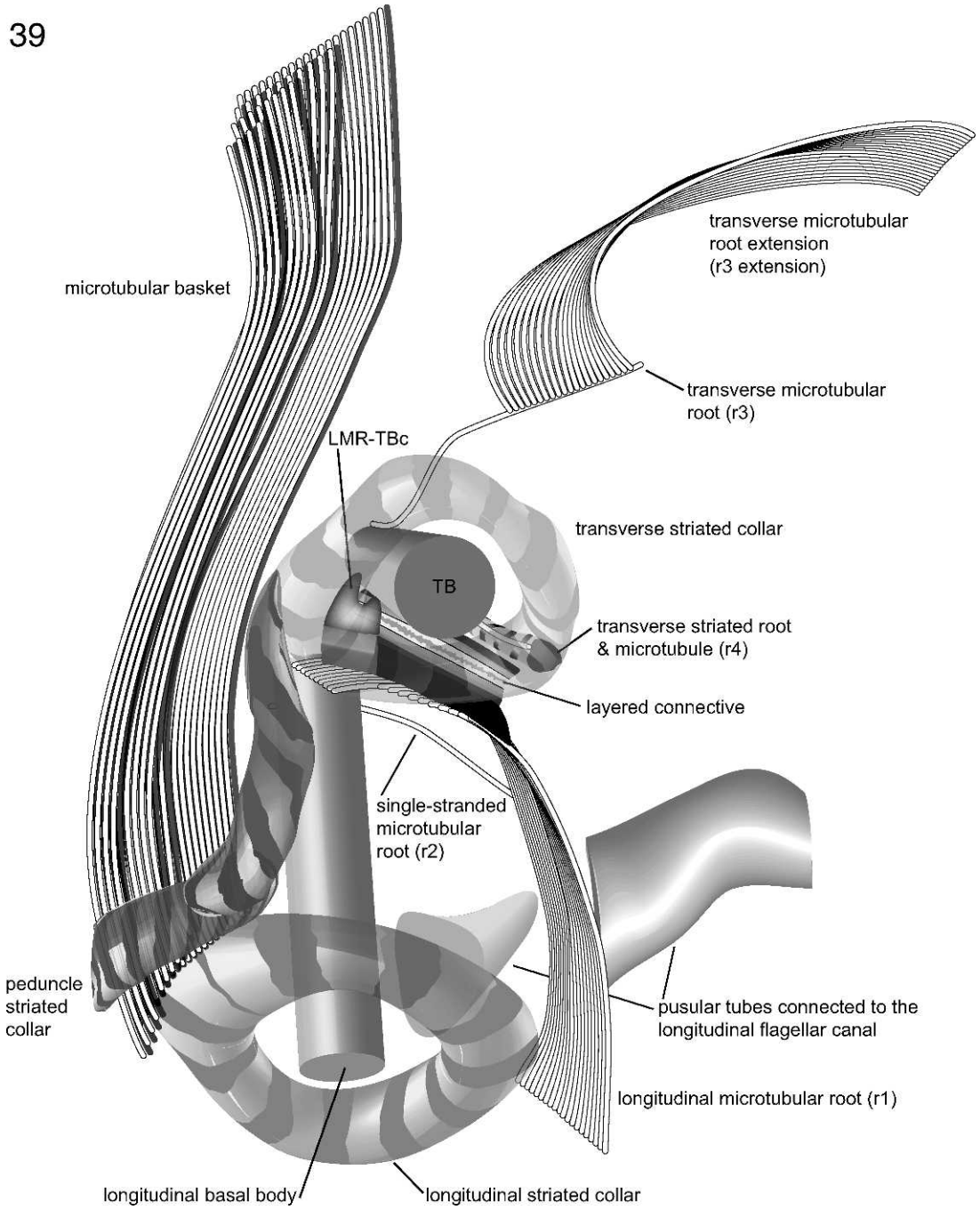

Fig. 39. Schematic reconstruction of the flagellar base area of *Theleodinium calcisporum*, viewed from the cell's left. The transverse and longitudinal striated collars, surrounding the exits points of the flagella, are rendered transparent to allow visualization of underlying structures. LMR-TBc, fibrous connective between the longitudinal microtubular root (root 1) and the transverse basal body.

striated collars (TSC), respectively (Figs 40–41, 46–48). There were four roots associated with the basal bodies, two with each one. The single-stranded microtubular root (SMR, designated r2 in Moestrup 2000) associated obliquely with the anterior-right side of the LB, curved to the dorsal side and toward the antapex of the cell (Figs 39, 42–43). A row of microtubules, the longitudinal microtubular root (LMR, r1 in Moestrup 2000) associated with the anterior-left side of the LB and extended roughly parallel to the SMR/r2 toward the antapex, passing near the LSC (Figs 39, 41, 44–47). The LMR/r1 comprised about nine microtubules in its proximal, anterior end, and the number increased distally, reaching some 20 microtubules in the sulcal region (Fig. 39). The dorsal face of the LMR/r1 at its proximal end was linked by a two-layered fibre to the proximal, posterior surface of the TB. This connective, designated LMR-TBc, was made of one electron-opaque, 80-nm thick layer that coated the LMR/r1 microtubules over an area of roughly 230 nm by 200 nm and was itself covered by a layer with a more fibrous appearance about 100 nm thick that contacted two adjacent triplets of

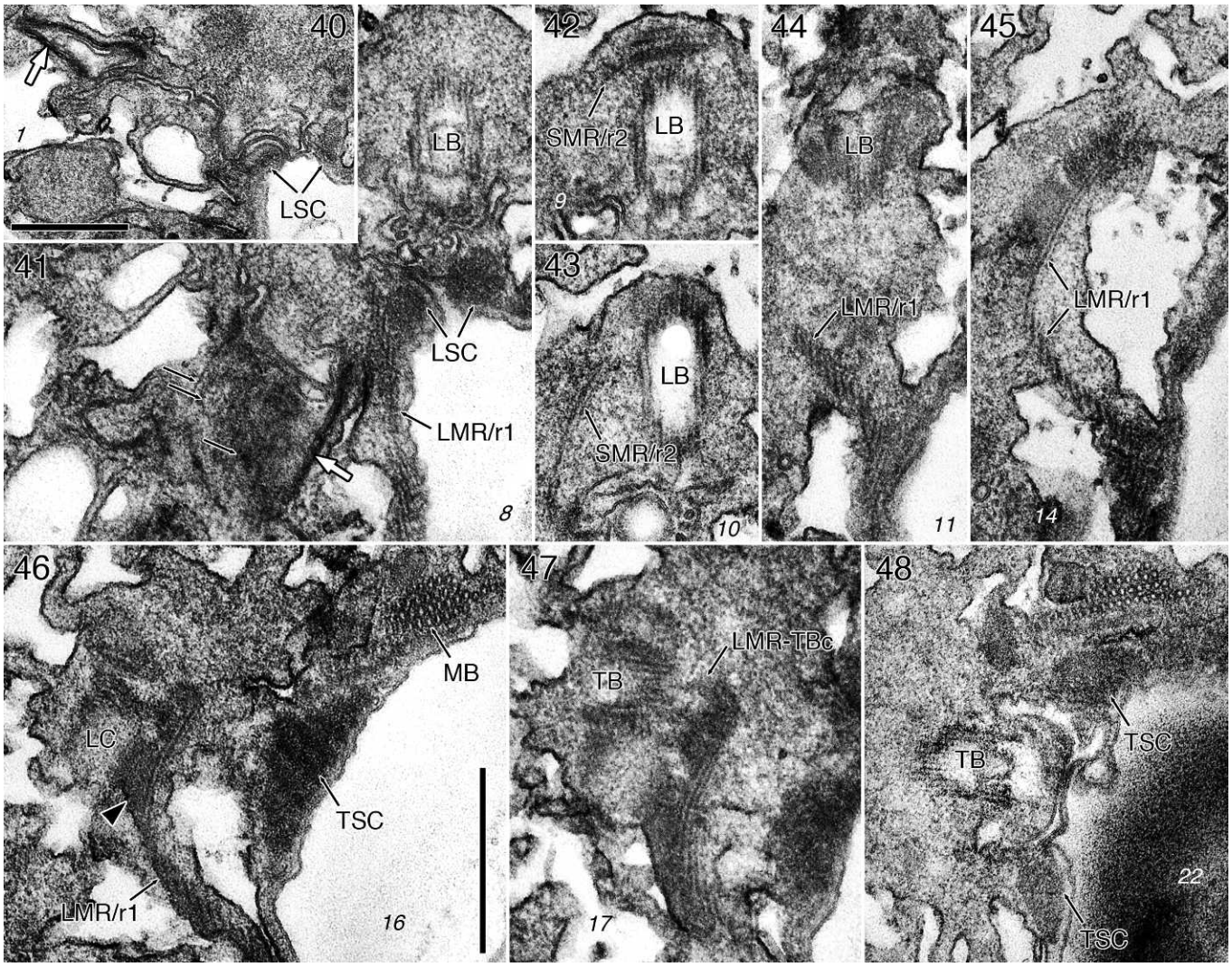

Figs 40–48. *Theleodinium calcisporum*, flagellar apparatus, TEM. Slanted numbers represent section numbers. Non-adjacent serial sections proceeding toward the left-apical side of the cell (viewed from the right-antapical end). Scale bars = 500 nm.

Fig. 40. A pusular tube (white arrow) is seen near the collapsed longitudinal flagellar canal and longitudinal striated collar (LSC).

Fig. 41. Another type of tube (white arrow), covered by parallel micro-fibrillar structures (thin arrows), near the collapsed longitudinal flagellar canal. LB, longitudinal basal body; LMR/r1, Longitudinal microtubular root (root 1); LSC, longitudinal striated collar. Same scale as Fig. 46.

Figs 42–43. Single-stranded microtubular root (SMR/r2) on the right side of the longitudinal basal body (LB). Same scale as Fig. 46.

Figs 44–48. The longitudinal basal body (LB) disappears and the longitudinal microtubular root (LMR/r1) is seen with some electron-opaque material on its dorsal side (arrowhead in Fig. 46). The layered connective (LC) appears on the dorsal side of the LMR between the electron-opaque material and the transverse basal body (TB). A connective is present between the proximal part of the LMR/r1 and the TB (LMR/r1-TBc). Four parallel rows of microtubules forming the microtubular basket (MB) are seen close to the transverse striated collar (TSC). All to the same scale.

the TB (Figs 39, 47, 51). Posterior and nearly adjacent to the LMR-TBc a layer of electron-opaque material coated the dorsal face of the LMR/r1, providing a wide connection with the posterior face of the so-called layered connective (LC) (Figs 39, 46–47, 50–52). The LC was nearly 800 nm long and 130 nm thick. As seen in almost cross-section, obtained through extensive tilting in the microscope, the LC was composed of two external electron-opaque layers about 30 nm thick (Figs 52–54) and three internal electron-transparent layers, each 35 nm thick, separated by two parallel, very thin, dark layers (Figs 52–54).

A single-stranded transverse microtubular root (TMR, r3 in Moestrup 2000) extended from the anterior-proximal side of the TB, curving toward the apex along the transverse flagellar canal (TFC), next to a row of collared pits (Figs 39, 49–51). Some 300 nm from the TB the TMR/r3 nucleated an extension of about 25 microtubules (labelled TMRE) that extended along the anterior side of the TFC. A second root connected with the TB was the so-called transverse striated root (TSR) and its associated microtubule (TSRM, r4 in Moestrup 2000). The proximal end of the TSRM/r4 associated with the anterior layer of the LC and the

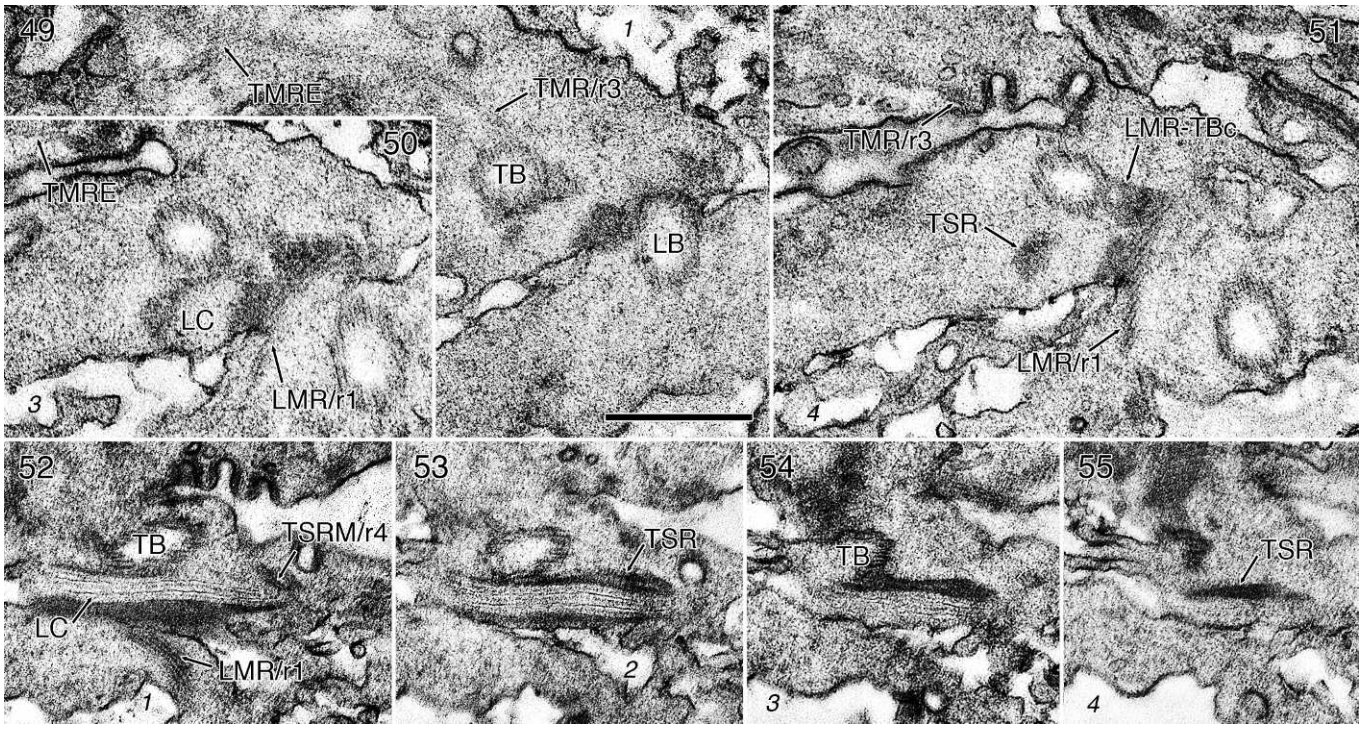

Figs 49–55. *Theleodinium calcisporum*, details of the flagellar apparatus, TEM. Slanted numbers represent section numbers. All to the same scale. Scale bar = 500 nm.

Figs 49–51. Non-adjacent, longitudinal serial sections viewed from the right-dorsal side of the cell. The transverse microtubular root (TMR/r3) is seen close to the proximal end of the transverse basal body (TB) in Fig. 49 and extends toward a row of collared pits. The transverse microtubular root extension (TMRE) is also visible. The transverse striated root (TSR) is seen close to the TB. LB, longitudinal basal body; LC, layered connective; LMR/r1, longitudinal microtubular root; LMR-TBc, fibrous connective between the longitudinal microtubular root (root 1) and the transverse basal body.

Figs 52–55. Adjacent serial sections that were tilted to show the aspect of the layered connective (LC) when in transverse section. The transverse striated root (TSR), with the transverse striated root microtubule (TSRM/r4), is attached to the anterior side of the LC. LMR/r1, longitudinal microtubular root; TB, transverse basal body.

proximal-posterior end of the TB, from where it extended to the left of the cell for about 500 nm (Figs 49–55).

Longitudinal sections through the ventral area showed the peduncle, a small cytoplasmic extension limited by a single membrane and surrounded in the exit point by a complete ring of fibrous material (peduncle striated collar, PSC) (Figs 56, 57). The PSC was located to the left of the striated collar of the longitudinal flagellum (LSC) and connected with the flagellar collars through striated collar extensions (Fig. 39). Four parallel rows of microtubules formed the microtubular basket (MB). From the PSC area the MB extended ventrally to the anterior left side of the cell for nearly 80 sections (about 6 μm) passing near an accumulation body (Figs 56–59). In a more internal and apical position, the MB was accompanied by elongated, electron-opaque vesicles on one side and by elongated, more transparent and slender vesicles on the other (Fig. 59). A transverse section of the MB, near the exit point, showed a total of 46 microtubules arranged in four parallel rows of four to 24 microtubules (Fig. 60).

Phylogeny of *Theleodinium calcisporum*

The phylogenetic backbone (i.e. the deep branches in the dinoflagellate tree) more or less formed a polytomy (see complete phylogenetic tree in Fig. S1) with no support from posterior probabilities (pp < 0.5) and bootstrap values (BS $<$ 50%). This was in contrast to many of the dinoflagellate lineages at the systematic level of orders and below. A subset of this phylogenetic tree containing only the closest relatives of the species of interest to this study, *Theleodinium calcisporum,* is shown in Fig. 61. *Theleodinium calcisporum,* together with *Duboscquodinium collinii*, *Scrippsiella sweeneyae* A.R. Loeblich and *Scrippsiella trochoidea* formed a highly supported sister group to *Tintinnophagus acutus* Coats (pp = 1.0 and BS = 100%). The relationship between *Duboscquodinium* and *Scrippsiella* spp. received no statistical support in the analyses conducted here (pp = 0.69 and BS $<$ 50%). The clade with *Tintinnophagus*, *Theleodinium* and *Scrippsiella* spp. (labelled clade 1 in Fig. 61) formed a sister group to a large clade containing *Thoracosphaera*, *Peridinium aciculiferum* Lemmermann and the pfiesteriaceans (i.e. *Stoeckeria* sp., *Pfiesteria* spp., *Cryptoperidiniopsis* spp. and *Luciella* spp.), labelled clade 2 in Fig. 61. This relationship received maximum support in posterior probability and good support in ML bootstrap value (BS = 81%). It should be noted that the tree topology obtained from Bayesian analysis of the partitioned data did not differ significantly from that obtained with a non-partitioned setting (data not shown).

The topology obtained using a Bayesian approach to infer the phylogeny of *Theleodinium calcisporum* on the basis of ITS 1, 5.8 S rDNA and ITS 2 is shown in Fig. 62. *Theleodinium* formed a sister taxon to *Scrippsiella donghaiensis* but this

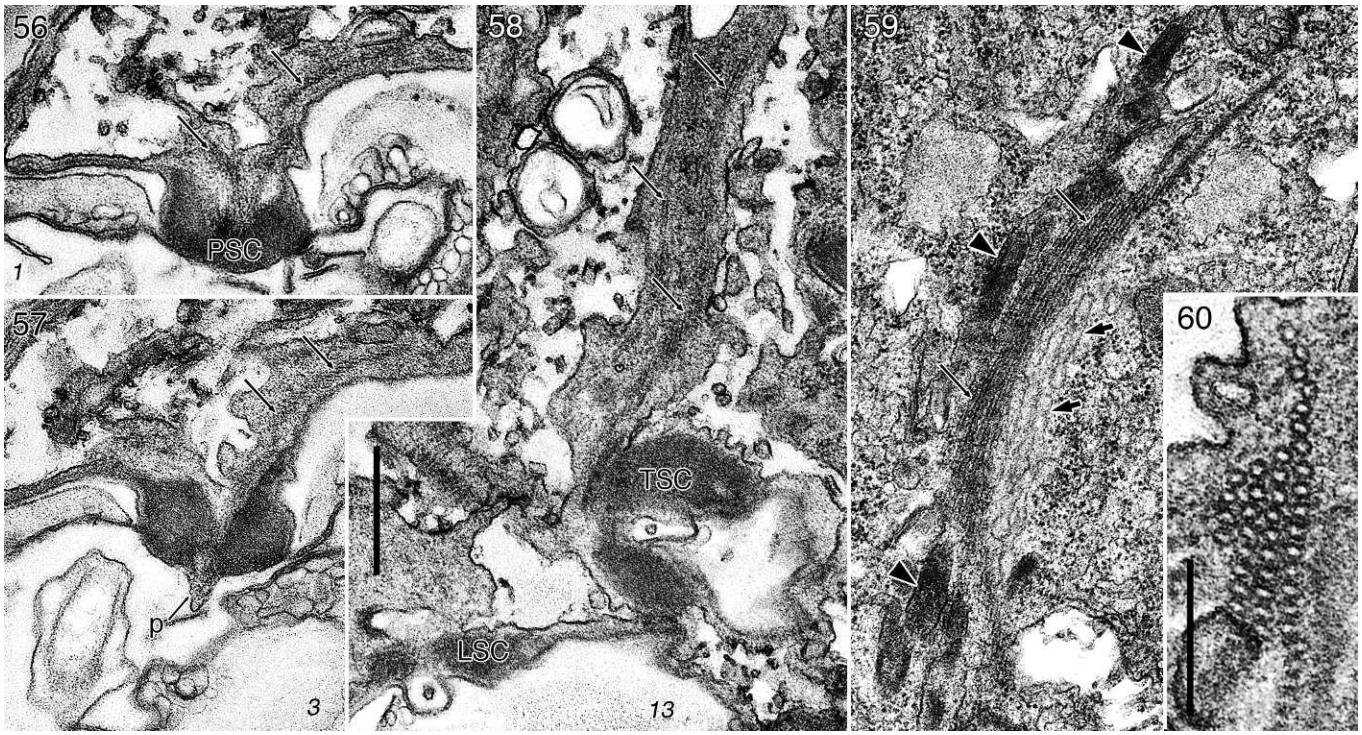

Figs 56–60. *Theleodinium calcisporum*, peduncle and microtubular basket, TEM.
Figs 56–58. Non-adjacent serial sections proceeding from ventral to dorsal, showing a complete collar (PSC) around the base of a small peduncle (p), and the collars for the transverse (TSC) and longitudinal (LSC) basal bodies. Rows of microtubules are marked with thin arrows. Slanted numbers represent section numbers. Scale bar = 500 nm.
Fig. 59. Microtubular basket seen in a more internal position in the cell (ca. 5.5 μm from the area of emergence of the peduncle). The microtubules (thin arrows) are seen parallel to several elongated vesicles (arrowheads) and lighter elongated vesicles (short arrows). Same scale as Fig. 58.
Fig. 60. Transverse section through the microtubular basket near the emergence point from the cell, with four parallel rows of microtubules. Scale bar = 200 nm.

relationship received little statistical support from Bayesian analysis (pp = 0.65) and BS < 50% in maximum likelihood analyses. Rather *Theleodinium* was part of an assemblage of species assigned to the *Scrippsiella* (viz. *Scrippsiella rotunda* and *Scrippsiella infula*) and *Calciodinellum* (viz. *Calciodinellum albatrosianum* and *Calciodinellum operosum*). This lineage was highly supported in Bayesian analysis (pp = 0.99) but not in maximum likelihood (BS < 50%). In fact the tree topology of the deepest branches received low statistical support (particularly in maximum likelihood bootstrap analyses) and thus formed a polytomy. However, *Theleodinium calcisporum* did seem to constitute a distinct lineage within this unresolved tree, as it did not group strongly with any of the included species of *Scrippsiella*.

The sequence divergence estimated for species included within clade 1 and *Thoracosphaera* of clade 2 (Figs 61 and S1 online) varied between 1.9% for the pair *Scrippsiella sweeneyae* (HQ845331)–*Scrippsiella* "*trochoidea*" (HM483396) and 13.3% for *Thoracosphaera heimii* (HQ845327)–*Tintinnophagus acutus* (HM483397) when based on Kimura-2-p distances (data not shown). Among the pairwise comparisons *Theleodinium calcisporum* had its highest sequence divergence to *Thoracosphaera heimii* (10.8%) and its lowest divergence to *Duboscquodinium collinii* (HM483398) (3.8%), again based on Kimura-2-p distances. These sequence divergence estimates were based a total of 3068 nucleotides including internal gaps.

DISCUSSION

The typical epithecal tabulation found in *Theleodinium calcisporum*, with an elongate apical plate 2 that curves around the apical pore, is very unusual and has no match among regular tabulation types of freshwater dinoflagellate species. However, in a discussion about tabulation variability in peridinioids, Lindemann (1926, fig. 9) depicted a plate arrangement just like that of *Theleodinium calcisporum*, which he interpreted as one of several tabulation variants of the species *Staszicella dinobryonis* Wołoszyńska. The genus *Staszicella* Wołoszyńska was originally separated from other armoured dinoflagellates on the basis of the smaller epicone relative to the hypocone (Wołoszyńska 1916, 1917). The epithet of the only described species of *Staszicella* alludes to the tendency of the cells to form non-motile stages attached to the loricae of *Dinobryon* (Chrysophyceae) species by means of mucilage secreted from a wide apical pore complex (Wołoszyńska 1916). The typical tabulation illustrated by Wołoszyńska (1916, pl. 12, fig. 40) displayed an asymmetrical arrangement of five apical plates surrounding a remarkably large pore complex, a single square-rhomboid anterior intercalary and seven precingular plates. The representation of an abnormal epithecal tabulation (Wołoszyńska 1917, pl. 12, fig. 27) seems to have originated an unwarranted idea that the taxon is unusually variable in

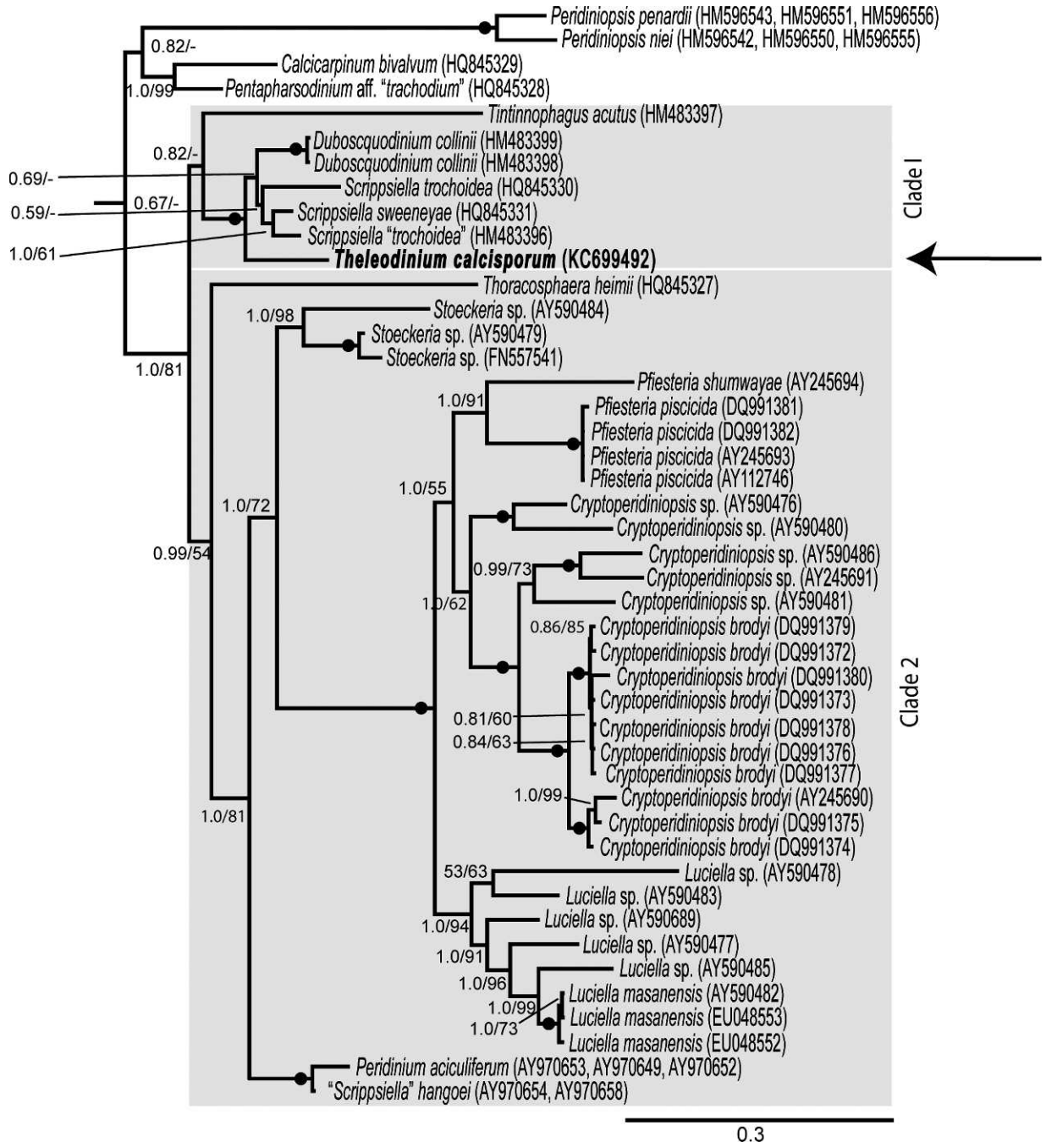

Fig. 61. Portion of a molecular phylogeny of dinoflagellates to show the position of *Theleodinium calcisporum* (arrow) based on an alignment that comprised 4620 nucleotides (including introduced gaps). It was originally compiled by Gottschling *et al*. (2012) and included nuclear encoded ribosomal genes (SSU, 5.8S and partial LSU rDNA) and intergenic spacer regions (ITS 1 and 2). The tree topology was obtained from Bayesian analysis and the outgroup taxa consisted of three apicomplexans and *Perkinsus* spp. Branch support values given at internodes are from posterior probabilities (≥ 0.5) and maximum likelihood bootstrapanalyses with 500 replications ($\geq 50\%$). Maximum branch support (posterior probability = 1 and 100% in ML bootstrap) is indicated by filled black circles. Branch lengths are proportional to the number of character changes. Only the clades containing the closest relatives of *Theleodinium calcisporum* are shown here. The complete molecular phylogeny is shown in supplemental material as Fig. S1.

plate arrangement, despite Wołoszyńska's (1917) statement that the number of plates is constant. Lindemann (1926) reported on populations with equal-sized epi- and hypocones that occasionally attached to *Dinobryon* and elaborated on the purported tabulation variability to interpret a number of variants in epithecal plate dispositions as derived from *Staszicella dinobryonis* typical plate arrangement. The variants were apparently reported from several different populations (Lindemann 1926), which diverged more or less significantly from *Staszicella dinobryonis* tabulation and showed a notably smaller apical pore complex. The typical features described for *Staszicella dinobryonis*, including the

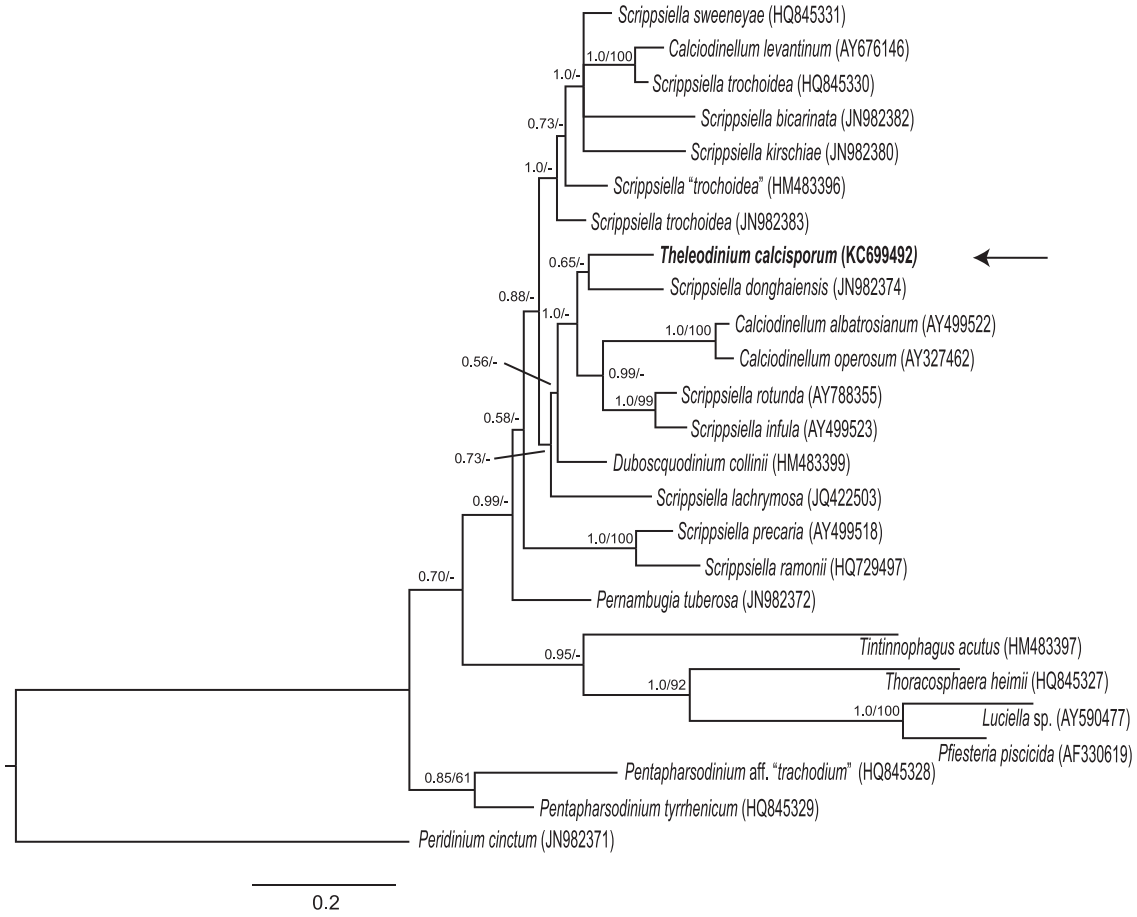

Fig. 62. Molecular phylogeny of dinoflagellates to show the position of *Theleodinium calcisporum* (arrow) based on complete ITS region (including 5.8S rDNA) and inferred from Bayesian analysis. Clustal W was used to generate the alignment, which included 655 nucleotides including introduced gaps, for 25 dinoflagellates. *Peridinium cinctum* (Peridiniales) constituted the outgroup. Posterior probabilities (pp values ≥ 0.5) from Bayesian analyses and bootstrap values (BS $\geq 50\%$) from maximum likelihood analyses are written at internodes. If lower than these values the branch support was indicated by "-". The branch lengths are proportional to the number of changes per site.

large pore complex, have recently been documented by modern methods in populations from the Trentino Province, Italy (Hansen & Flaim 2007). Lindemann's (1926) variations represent therefore one or several species but are unlikely to be *Staszicella dinobryonis*. As Lindemann did not describe the cell contents it is uncertain whether he depicted the species we report on; there was no mention of an apical protuberance in any of the cells and the tabulation type we found in about 13% of the cells, with four symmetrically arranged apical and two intercalary plates, was not among the variants he described (Lindemann 1926).

Our cultures of *Theleodinium calcisporum* did not approach the morphology, tabulation or shape of the apical complex of *Staszicella dinobryonis* as described by Wooszyńska (1916, 1917) and Hansen & Flaim (2007). Moreover, the numerous yellowish-brown chloroplast lobes that were evident along the surface of *Theleodinium calcisporum* cells, some distinctly associated with pyrenoids, contrast with Wołoszyńska's (1916) statement that the chloroplasts were difficult to detect, a difficulty shared by Hansen & Flaim (2007), who hypothesized that *Staszicella dinobryonis* may actually be colourless from the analysis of fixed material.

The cells of *Theleodinium calcisporum* showed a typical dinoflagellate fine-structural organization with a regular dinokaryon and chloroplast lobes with the membrane arrangements usual in peridinin-containing species. The presence of stacks of more than three thylakoids in several chloroplast lobes of *Theleodinium calcisporum*, some of which resembled pseudo-grana, is uncommon in dinoflagellates; although, regular grana formation has been shown in *Gonyaulax spinifera* (Claparède & J. Lachmann) Diesing (Hansen *et al*. 1996). Both the physiological and the phylogenetic significance of these elaborate thylakoid stacks in dinoflagellates are unknown.

Although the pore plate of *Theleodinium calcisporum* is unusually elevated the features observed in the apical fibrous complex are the usual for this type of structure (Roberts *et al*. 1987). However, the amphiesmal vesicle profiles without plate material observed between the pore and cover plates of *Chimonodinium lomnickii*, *Scrippsiella trochoidea*, *Scrippsiella sweeneyae* and *Heterocapsa pygmaea* A.R. Loeblich, R.J. Schmidt & Sherley (Roberts *et al*. 1987; Craveiro *et al*. 2011) were not found in *Theleodinium calcisporum*.

An eyespot of type A, formed by osmiophilic globules located in a chloroplast lobe in the sulcal area (Moestrup &

Daugbjerg 2007; Craveiro *et al*. 2010) is common in autotrophic peridinioids, e.g. *Peridinium cinctum*, *Chimonodinium lomnickii* and *Scrippsiella trochoidea* (Calado *et al*. 1999; Craveiro *et al*. 2011) and was therefore expected in our material. However, it was not visible in light microscopy and it was not detected in TEM; although, the ventral area of five cells was examined in serial sections.

Comparison with non-calcareous peridinioids

The reconstruction of the flagellar apparatus of several peridinioids has disclosed a number of features that seem to be characteristic of the group. A single-stranded microtubular root associated with the right side of the longitudinal basal body (r2, SMR) and a layered connective (LC) between the longitudinal microtubular root (r1, LMR) and the transverse basal body have been found in all peridinioids studied in detail (Calado *et al*. 1999; Calado & Moestrup 2002; Calado *et al*. 2009; Craveiro *et al*. 2009; Craveiro *et al*. 2011). Although the LC was found only in peridinioids the r2/SMR was also found in gonyaulacoids and in *Baldinia anauniensis* Gert Hansen & Daugbjerg (Hansen & Moestrup 1998; Hansen *et al*. 2007). Unsurprisingly, these two features are present in the flagellar apparatus of *Theleodinium calcisporum*, which shows greater overall similarity to the homologous area of *Chimonodinium lomnickii* than to any other basal body region known in detail (Craveiro *et al*. 2011). A notable difference is the absence in *Theleodinium calcisporum* of the association of a fibre with the transverse microtubular root extension (TMRE), as seen in *Chimonodinium lomnickii* (Craveiro *et al*. 2011). The significance of this fibre-microtubular root association, which was found most developed in *Peridiniopsis borgei* (Calado & Moestrup 2002), is unknown.

The resemblance between the flagellar base regions of *Theleodinium calcisporum* and *Chimonodinium lomnickii* extends to the microtubular basket (MB), which shows essentially similar paths and number of rows of microtubules in both species (Craveiro *et al*. 2011). The presence of a MB suggests phylogenetic relationship with the pfiesteriaceans, which use a more extensive version of this microtubular structure to feed (Litaker *et al*. 2002; Calado *et al*. 2009). Although previously thought to comprise only marine species, the pfiesteriaceans are represented in freshwater by *Tyrannodinium edax* (A.J. Schilling) Calado, a widespread and common species previously referred to as *Peridiniopsis berolinensis* (Lemmermann) Bourrelly (Wedemayer & Wilcox 1984; Calado & Moestrup 1997; Calado 2011). In contrast to the feeding cells of the pfiesteriaceans, which have no lasting functional chloroplasts, both *Theleodinium calcisporum* and *Chimonodinium lomnickii* are photosynthetic and have not been shown to use their MB.

Other peridinioids that are not members of the Thoracosphaeraceae sensu Elbrächter *et al*. (2008) are not known to possess a MB. In *Palatinus apiculatus* (Ehrenberg) Craveiro, Calado, Daugbjerg & Moestrup a single, apparently reduced, microtubular strand (usually labelled MSP) is present in a position homologous to the MB location (Craveiro *et al*. 2009). No microtubular system homologous to a MB or MSP was found in *Peridinium cinctum* (Calado *et al*. 1999). Both *Peridinium* and *Palatinus* lack an apical pore complex and each presents differences in thecal and internal cell organization (see discussion in Craveiro *et al*. 2011). In *Peridiniopsis borgei* a single strand of 75–80 microtubules extended for over 20 μm from a small, flat peduncle to the left side of the cell and progressively divided into two and then four strands that continued toward the dorsal part of the cell (Calado & Moestrup 2002). This peculiar microtubular system, of unknown function, is accompanied by *Peridiniopsis borgei*'s unusual tabulation, with three apical plates and a single anterior intercalary plate in a bilaterally symmetrical disposition, and an internal cell organization with a unique combination of a large sac pusule connected to the longitudinal flagellar canal and a single, large, dorsal pyrenoid enveloped by starch (Calado & Moestrup 2002).

As shown above, *Theleodinium calcisporum* appears close to *Chimonodinium lomnickii* in several aspects. However, the two species differ in the following points: *Chimonodinium lomnickii* has an epithecal tabulation with four apical and three intercalary plates, possesses a large eyespot, has no defined pyrenoids and its pusular system is formed by two well-defined tubes, each connected to one flagellar canal (Craveiro *et al*. 2011).

Comparison with other calcareous peridinioids

The capability of producing calcareous cysts is the most intriguing feature of *Theleodinium calcisporum*. Until now, this characteristic was known only from marine dinoflagellates. The production of calcareous cell covers has been considered an apomorphy of the Thoracosphaeraceae, a family that includes also non-calcareous species, which are presumed to have secondarily lost this feature (Gottschling *et al*. 2012). Genera that produce calcareous cysts or coccoid stages during their life cycle (e.g. *Scrippsiella*, *Calciodinellum* Deflandre, *Calcigonellum* Deflandre, *Calcicarpinum* Deflandre, *Pentapharsodinium* Indelicato & A.R. Loeblich, *Pernambugia* Janofske & Karwath) have motile stages with similar epithecal tabulation: pp, cp, x, 4′, 3a, 7′′. Small differences occur in a few *Scrippsiella* species, with intercalary plates 1a and 3a abutting each other instead of the usual disposition in a row of the intercalary plates (Montresor & Zingone 1988; Montresor 1995; Gottschling *et al*. 2005b). A significant difference occurs in the number of cingular plates of *Pentapharsodinium*, which are five rather than the usual six (one small, so-called transitional, plus five) found in other genera (D'Onofrio *et al*. 1999). *Theleodinium calcisporum* approaches the *Scrippsiella* group in having six cingular plates (T + 5); although, its epithecal tabulation is quite distinct.

The morphology of calcareous cysts is diverse and often complements, or even fundaments, discrimination of species with very similar motile stages (e.g. Zinssmeister *et al*. 2012). High variability in cyst morphology has also been reported within strains of calcareous dinoflagellates (Gottschling *et al*. 2005b). Cysts of *Theleodinium calcisporum* varied in the extent of the calcified layer and in crystal shape. The *Theleodinium* cysts with cubic, scattered crystals represented on Figs 22–24 are reminiscent of the one described by Montresor *et al*. (2003, fig. 28) as a variation in a strain of *Scrippsiella trochoidea*. It appears possible that these types represent an early stage of cyst formation as in both cases cysts with larger crystals forming a more complete envelope were also found (Montresor *et al*. 2003).

The prominent starch-enveloped pyrenoids present in *Theleodinium calcisporum* suggest proximity to the group of organisms with calcareous cysts, as starch-enveloped pyrenoids are a regular feature of *Scrippsiella* species, and also of *Calciodinellum* and *Calcigonellum* (D'Onofrio *et al*. 1999). Pyrenoids adjacent to starch grains have recently been reported also in *Leonella granifera* (D. Fütterer) Janofske & Karwath, *Thoracosphaera heimii* and *Pernambugia tuberosa* (Zinssmeister *et al*. 2013).

Fine-structural comparison between *Theleodinium calcisporum* and *Scrippsiella* (as represented by *Scrippsiella trochoidea*; see Craveiro *et al*. 2011) reveals a rather similar general organization of the motile cell but also exposes some important differences. One is the presence of a relatively small eyespot in *Scrippsiella trochoidea*. Another difference is the pusular system of *Scrippsiella trochoidea*, with tubular or flattened, ramified vesicles concentrated on a large portion of the right mid-ventral cytoplasm. Perhaps more significant are the canals formed by what seem to be supernumerary plates at the exit point of the flagella of *Scrippsiella trochoidea* (Craveiro *et al*. 2011). However, the most striking difference is the absence of any microtubular system that could be considered homologous to a MB or MSP in *Scrippsiella*, as determined in four cells of *Scrippsiella trochoidea* examined in serial sections (Craveiro *et al*. 2011), and corroborated by published SEM images of *Scrippsiella* species, which do not show an emergent peduncle (contrast with the peduncle of *Theleodinium calcisporum*, visible in Fig. 1).

In summary, the fine structure of *Theleodinium calcisporum* places it in an intermediate position between *Scrippsiella* and *Chimonodinium*. In having two characters that are presumably ancestral in the group, viz. the production of calcareous cysts and the MB, *Theleodinium* appears closer to the common ancestor of *Scrippsiella* and *Chimonodinium*. However, from the *Scrippsiella* and *Chimonodinium* lineages, which have a similar plate organization, it diverged in tabulation; and it diverged from the *Scrippsiella* lineage in habitat.

Molecular phylogeny

The most inclusive phylogenetic tree (Figs 61 and S1 online) shows *Theleodinium* in a statistically supported clade together with species of *Scrippsiella* and *Duboscquodinium collinii*. This clade in turn appears as a sister group to *Tintinnophagus acutus*; although, with no statistical support. The close relationship between *Scrippsiella* species and the parasitic *Duboscquodinium collinii*, and the association of this group with *Tintinnophagus acutus* has been previously retrieved by Coats *et al*. (2010) and Gottschling *et al*. (2012). Current knowledge on the structure and lifestyle of *Duboscquodinium collinii* is insufficient to provide phenotypic characters that may explain the affinities suggested in this phylogenetic hypothesis (Coats *et al*. 2010; 2012). On the other hand, some scrippsielloid features were demonstrated for the dinospore of *Tintinnophagus acutus*; there is a projecting apical pore and thecal plates seem to be present (Coats *et al*. 2010). Consistent with its parasitic (predatory) nature a peduncle was shown by SEM in *Tintinnophagus* (Coats *et al*. 2010), suggesting the presence of a MB. This represents another assortment of characters in what appears to be a remarkably variable clade. The placement of *Theleodinium calcisporum* in this clade is compatible with its combination of *Scrippsiella* features (e.g. general cell organization, with chloroplasts and pyrenoids, and production of calcareous cysts) with the retention of the feeding apparatus (i.e. the MB, with its associated vesicles and a ring of fibrous material surrounding the exit point of a peduncle).

The topology of the tree based on ITS-5.8S rDNA (Fig. 62) is generally compatible with that shown in Figs 61 and S1 (online); although, most branches received little or no statistical support. The two clades shown in Zinssmeister *et al*. (2012) with species currenty classified in *Scrippsiella* and *Calciodinellum* are retrieved in the present ITS tree, with *Theleodinium* associated with the clade not containing typical *Scrippsiella* species (*Scrippsiella sweeneyae*, *Scrippsiella trochoidea*). In view of the differences in fine structural features between *Theleodinium* and those reported for *Scrippsiella trochoidea* (Craveiro *et al*. 2011) it appears interesting to examine the ultrastructure of species in the clade that contains the new genus.

The genus *Chimonodinium*, not included in our trees for lack of ITS sequence data, has been shown in previously published phylogenetic trees based on SSU and on LSU rDNA to group with the pfiesteriacean clade, close to the branching point of *Peridinium aciculiferum* (see Craveiro *et al*. 2011). This is compatible with the picture given by the structural analysis, that *Theleodinium* occupies an intermediate evolutionary position between the *Scrippsiella* clade and the clade containing *Chimonodinium* and the pfiesteriaceans.

ACKNOWLEDGEMENTS

SCC was supported by a grant (SFRH/BPD/68537/2010) from the financing program "QREN - POPH - Tipologia 4.1 - Formação Avançada" and by the European Social Funding (FSE) and the Portuguese Ministry of Education and Science (MEC).

SUPPLEMENTARY DATA

Supplementary data associated with this article can be found online at http://dx.doi.org/10.2216/13–152.1.s1.

REFERENCES

Calado A.J. 2011. On the identity of the freshwater dinoflagellate *Glenodinium edax*, with a discussion on the genera *Tyrannodinium* and *Katodinium*, and the description of *Opisthoaulax* gen. nov. *Phycologia* 50: 641–649.

Calado A.J. & Moestrup Ø. 1997. Feeding in *Peridiniopsis berolinensis* (Dinophyceae): new observations on tube feeding by an omnivorous, heterotrophic dinoflagellate. *Phycologia* 36: 47–59.

Calado A.J. & Moestrup Ø. 2002. Ultrastructural study of the type species of *Peridiniopsis*, *Peridiniopsis borgei* (Dinophyceae), with special reference to the peduncle and flagellar apparatus. *Phycologia* 41: 567–584.

Calado A.J., Hansen G. & Moestrup Ø. 1999. Architecture of the flagellar apparatus and related structures in the type species of *Peridinium*, *P. cinctum* (Dinophyceae). *European Journal of Phycology* 34: 179–191.

Calado A.J., Craveiro S.C., Daugbjerg N. & Moestrup Ø. 2009. Description of *Tyrannodinium* gen. nov., a freshwater dinoflagellate closely related to the marine *Pfiesteria*-like species. *Journal of Phycology* 45:1195–1205.

Carty S. 2008. *Parvodinium* gen. nov. for the Umbonatum group of *Peridinium* (Dinophyceae). *Ohio Journal of Science* 108: 103–107.

Coats D.W., Kim S., Bachvaroff T.R., Handy S.M. & Delwiche C.F. 2010. *Tintinnophagus acutus* n. g., n. sp. (Phylum Dinoflagellata), an ectoparasite of the ciliate *Tintinnopsis cylindrica* Daday 1887, and its relationship to *Duboscquodinium collini* Grassé 1952. *Journal of Eukaryotic Microbiology* 57: 468–482.

Coats D.W., Bachvaroff T.R. & Delwiche C.F. 2012. Revision of the family Duboscquellidae with description of *Euduboscquella crenulata* n. gen., n. sp. (Dinoflagellata, Syndinea), an intracellular parasite of the ciliate *Favella panamensis* Kofoid & Campbell, 1929. *Journal of Eukaryotic Microbiology* 59: 1–11.

Craveiro S.C., Calado A.J., Daugbjerg N. & Moestrup Ø. 2009. Ultrastructure and LSU rDNA-based revision of *Peridinium* group palatinum (Dinophyceae) with the description of *Palatinus* gen. nov. *Journal of Phycology* 45: 1175–1194.

Craveiro S.C., Moestrup Ø., Daugbjerg N. & Calado A.J. 2010. Ultrastructure and large subunit rDNA-based phylogeny of *Sphaerodinium cracoviense*, an unusual freshwater dinoflagellate with a novel type of eyespot. *Journal of Eukaryotic Microbiology* 57: 568–585.

Craveiro S.C., Calado A.J., Daugbjerg N., Hansen G. & Moestrup Ø. 2011. Ultrastructure and LSU rDNA-based phylogeny of *Peridinium lomnickii* and description of *Chimonodinium* gen. nov. (Dinophyceae). *Protist* 162: 590–615.

Darriba D., Taboada G.L., Doallo R. & Posada D. 2012. jModelTest 2: more models, new heuristics and parallel computing. *Nature Methods* 9: 772.

Daugbjerg N., Moestrup Ø. & Arctander P. 1994. Phylogeny of the genus *Pyramimonas* (Prasinophyceae) inferred from the *rbc*L gene. *Journal of Phycology* 30: 991–999.

D'Onofrio G., Marino D., Bianco L., Busico E. & Montresor M. 1999. Toward an assessment on the taxonomy of dinoflagellates that produce calcareous cysts (Calciodinelloideae, Dinophyceae): a morphological and molecular approach. *Journal of Phycology* 35: 1063–1078.

Elbrächter M., Gottschling M., Hildebrand-Habel T., Keupp H., Kohring R., Lewis J., Meier K.J.S., Montresor M., Streng M., Versteegh G.J.M., Willems H. & Zonneveld K. 2008. Establishing an agenda for calcareous dinoflagellate research (Thoracosphaeraceae, Dinophyceae) including a nomenclatural synopsis of generic names. *Taxon* 57: 1289–1303.

Gao X. & Dodge J.D. 1991. The taxonomy and ultrastructure of a marine dinoflagellate, *Scrippsiella minima* sp. nov. *British Phycological Journal* 26: 21–31.

Gao X., Dodge J.D. & Lewis J. 1989. An ultrastructural study of planozygotes and encystment of a marine dinoflagellate, *Scrippsiella* sp. *British Phycological Journal* 24: 153–165.

Gottschling M., Keupp H., Plötner J., Knop R., Willems H. & Kirsch M. 2005a. Phylogeny of calcareous dinoflagellates as inferred from ITS and ribosomal sequence data. *Molecular Phylogenetics and Evolution* 36: 444–455.

Gottschling M., Knop R., Plötner J., Kirsch M., Willems H. & Keupp H. 2005b. A molecular phylogeny of *Scrippsiella sensu lato* (Calciodinellaceae, Dinophyta) with interpretations on morphology and distribution. *European Journal of Phycology* 40: 207–220.

Gottschling M., Soehner S., Zinssmeister C., John U., Plötner J., Schweikert M., Aligizaki K. & Elbrächter M. 2012. Delimitation of the Thoracosphaeraceae (Dinophyceae), including the calcareous dinoflagellates, based on large amounts of ribosomal RNA sequence data. *Protist* 163: 15–24.

Guindon S., Dufayard J.F., Lefort V., Anisimova M., Hordijk W. & Gascuel O. 2010. New algorithms and methods to estimate maximum-likelihood phylogenies: assessing the performance of PhyML 3.0. *Systematic Biology* 59: 307–321.

Hansen G. & Moestrup Ø. 1998. Fine-structural characterization of *Alexandrium catenella* (Dinophyceae) with special emphasis on the flagellar apparatus. *European Journal of Phycology* 33: 281–291.

Hansen G. & Flaim G. 2007. Dinoflagellates of the Trentino Province, Italy. *Journal of Limnol*ogy 66: 107–141.

Hansen G., Moestrup Ø. & Roberts K.R. 1996. Fine structural observations on *Gonyaulax spinifera* (Dinophyceae), with special emphasis on the flagellar apparatus. *Phycologia* 35: 354–366.

Hansen G., Daugbjerg N. & Franco J.M. 2003. *Alexandrium minutum* (Dinophyceae) from Denmark – a study based on morphology, toxin composition and LSU rDNA sequences, with some morphological observations on other European strains. *Harmful Algae* 2: 317–335.

Hansen G., Daugbjerg N. & Henriksen P. 2007. *Baldinia anauniensis* gen. et sp. nov.: a 'new' dinoflagellate from Lake Tovel, N. Italy. *Phycologia* 46: 86–108.

Inouye I. & Pienaar R.M. 1983. Observations on the life cycle and microanatomy of *Thoracosphaera heimii* (Dinophyceae) with special reference to its systematic position. *South African Journal of Botany* 2: 63–75.

Janofske D. 2000. *Scrippsiella trochoidea* and *Scrippsiella regalis,* nov. comb. (Peridiniales, Dinophyceae): a comparison. *Journal of Phycology* 36: 178–189.

Lindemann E. 1926. Bewegliche Hüllenfelderung und ihr Einflu auf die Frage der Artbildung bei Glenodinien. Spezielle Bemerkungen über die untersuchten Formen. Systematische Neuordnung bei niederen Peridineen. *Archiv für Hydrobiologie* 16: 437–458.

Lindström K. 1991. Nutrient requirements of the dinoflagellate *Peridinium gatunense*. *Journal of Phycology* 27: 207–219.

Litaker R.W., Vandersea M.W., Kibler S.R., Madden V.J., Noga E.J. & Tester P.A. 2002. Life cycle of the heterotrophic dinoflagellate *Pfiesteria piscicida* (Dinophyceae). *Journal of Phycology* 38: 442–463.

Logares R., Shalchian-Tabrizi K., Boltovskoy A. & Rengefors K. 2007. Extensive dinoflagellate phylogenies indicate infrequent marine-freshwater transitions. *Molecular Phylogenetics and Evolution* 45: 887–903.

Moestrup Ø. 2000. The flagellate cytoskeleton. Introduction of a general terminology for microtubular flagellar roots in protists. In: *The flagellates. Unity, diversity and evolution* (Ed. by B.S.C. Leadbeater & J.C. Green), pp. 69–94. Taylor & Francis, New York (Systematics Association Special Volume No. 59).

Moestrup Ø. & Daugbjerg N. 2007. On dinoflagellate phylogeny and classification. In: *Unravelling the algae, the past, present, and future of algal systematics* (Ed. by J. Brodie & J. Lewis), pp. 215–230. CRC Press, Boca Raton (Systematics Association Special Volume No. 75).

Montresor M. 1995. *Scrippsiella ramonii* sp. nov. (Peridiniales, Dinophyceae), a marine dinoflagellate producing a calcareous resting cyst. *Phycologia* 34: 87–91.

Montresor M. & Zingone A. 1988. *Scrippsiella precaria* sp. nov. (Dinophyceae), a marine dinoflagellate from the Gulf of Naples. *Phycologia* 27: 387–394.

Montresor M., Sgrosso S., Procaccini G. & Kooistra W.H.C.F. 2003. Intraspecific diversity in *Scrippsiella trochoidea* (Dinophyceae): evidence for cryptic species. *Phycologia* 42: 56–70.

Popovský J. & Pfiester L.A. 1990. Dinophyceae (Dinoflagellida). In: *Süsswasserflora von Mitteleuropa* (Ed. by H. Ettl, J. Gerloff, H. Heynig & D. Mollenhauer), vol. 6. G. Fisher, Jena. 272 pp.

Posada D. & Crandall K.A. 1998. Modeltest: testing the model of DNA substitution. *Bioinformatics* 14: 817–818.

Roberts K.R., Timpano P. & Montegut A.E. 1987. The apical fibrous complex: a new cytological feature of some dinoflagellates. *Protoplasma* 137: 65–69.

Ronquist F. & Huelsenbeck J.P. 2003. MrBayes 3: Bayesian phylogenetic inference under mixed models. *Bioinformatics* 19: 1572–1574.

Saldarriaga J.F., Taylor F.J.R., Cavalier-Smith T., Menden-Deuer S. & Keeling P.J. 2004. Molecular data and the evolutionary history of dinoflagellates. *European Journal of Protistol*ogy 40: 85–111.

Swofford D.L. 2002. PAUP* phylogenetic analysis using parsimony (*and other methods), version 4.0b10. Sinauer Associates, Sunderland, MA, USA.

Tangen K., Brand L.E., Blackwelder P.L. & Guillard R.R.L. 1982. *Thoracosphaera heimii* (Lohmann) Kamptner is a dino-

phyte: observations on its morphology and life cycle. *Marine Micropaleontology* 7: 193–212.

Wall D. & Dale B. 1968. Modern dinoflagellate cysts and evolution of the Peridiniales. *Micropaleontology* 14: 265–304.

Waterhouse A.M., Procter J.B., Martin D.M.A, Clamp M. & Barton, G.J. 2009. Jalview Version 2 – a multiple sequence alignment editor and analysis workbench. *Bioinformatics* 25: 1189–1191.

Wedemayer G.J. & Wilcox L.W. 1984. The ultrastructure of the freshwater colorless dinoflagellate *Peridiniopsis berolinense* (Lemm.) Bourrelly. *Journal of Protozoology* 31: 444–453.

White T.J., Bruns T., Lee S. & Taylor J.W. 1990. Amplification and direct sequencing of fungal ribosomal RNA genes for phylogenetics. In: *PCR Protocols: A Guide to Methods and Applications* (Ed. by M.A. Innis, D.H. Gelfand, J.J. Sninsky & T.J. White), pp. 315–322. Academic Press, Inc., New York.

Wołoszyńska J. 1916. Polskie Peridineae słodkowodne. — Polnische Süwasser-Peridineen. *Bulletin International de l'Academie des Sciences de Cracovie, Classe des Sciences Mathématiques et Naturelles, série B: Sciences Naturelles* 1915: 260–285, pls 10–14.

Wołoszyńska J. 1917. Nowe gatunki Peridineów, tudzież spostrzeżenia nad budową okrywy u Gymnodiniów i Glenodiniów. — Neue Peridineen-Arten, nebst Bemerkungen über den Bau der Hülle bei *Gymno-* und *Glenodinium*. *Bulletin International de l'Academie des Sciences de Cracovie, Classe des Sciences Mathématiques et Naturelles, série B: Sciences Naturelles* 1917: 114–122, pls 11–13.

Zinssmeister C., Soehner S., Facher E., Kirsch M., Meier K.J.S. & Gottschling M. 2011. Catch me if you can: the taxonomic identity of *Scrippsiella trochoidea* (F. Stein) A.R. Loebl. (Thoracosphaeraceae, Dinophyceae). *Systematics and Biodiversity* 9: 145–157.

Zinssmeister C., Soehner S., Kirsch M., Facher E., Meier K.J.S., Keupp H. & Gottschling M. 2012. Same but different: two novel bicarinate species of extant calcareous dinophytes (Thoracosphaeraceae, Peridiniales) from the Mediterranean sea. *Journal of Phycology* 48: 1107–1118.

Zinssmeister C., Keupp H., Tischendorf G., Kaulbars F. & Gottschling M. 2013. Ultrastructure of calcareous dinophytes (Thoracosphaeraceae, Peridiniales) with a focus on vacuolar crystal-like particles. *PLoS ONE* 8: e54038.

Zonneveld K.A.F., Meier K.J.S., Esper O., Siggelow D., Wendler I. & Willems H. 2005. The (palaeo-) environmental significance of modern calcareous dinoflagellate cysts: a review. *Paläontologische Zeitschrift* 79: 61–77.

Received 5 March 2013; accepted 8 July 2013
Associate Editor: Ken-ichiro Ishida